

2013

# Development of a quality assurance procedure for dose volume histogram analysis

David A. Davenport  
*The University of Toledo*

Follow this and additional works at: <http://utdr.utoledo.edu/theses-dissertations>

---

## Recommended Citation

Davenport, David A., "Development of a quality assurance procedure for dose volume histogram analysis" (2013). *Theses and Dissertations*. Paper 58.

This Thesis is brought to you for free and open access by The University of Toledo Digital Repository. It has been accepted for inclusion in Theses and Dissertations by an authorized administrator of The University of Toledo Digital Repository. For more information, please see the repository's [About](#) page.

A Thesis

entitled

Development of a Quality Assurance Procedure for Dose Volume Histogram Analysis

by

David A. Davenport

Submitted to the Graduate Faculty as partial fulfillment of the requirements for the

Master of Science in Biomedical Sciences Degree in Medical Physics

---

Dr. Diana Shyvdka, Committee Chair

---

Dr. E. Ishmael Parsai, Committee Member

---

Dr. David Pearson, Committee Member

---

Dr. Patricia R. Komuniecki, Dean

College of Graduate Studies

The University of Toledo

August 2013



An Abstract of  
Development of a Quality Assurance Procedure for Dose-Volume Histogram Analysis

by

David A. Davenport

Submitted to the Graduate Faculty as partial fulfillment of the requirements for the  
Master of Science in Biomedical Sciences Degree in Medical Physics

The University of Toledo

August 2013

The role of the dose-volume histogram (DVH) is rapidly expanding in radiation oncology treatment planning. DVHs are already relied upon to differentiate between two similar plans and evaluate organ-at-risk dosage. Their role will become even more important as progress continues towards implementing biologically based treatment planning systems. Therefore it is imperative that the accuracy of DVHs is evaluated and reappraised after any major software or hardware upgrades, affecting a treatment planning system (TPS). The purpose of this work is to create and implement a comprehensive quality assurance procedure evaluating dose volume histograms to insure their accuracy while satisfying American College of Radiology guidelines.

Virtual phantoms of known volumes were created in Pinnacle TPS and exposed to different beam arrangements. Variables including grid size and slice thickness were varied and their effects were analyzed. The resulting DVHs were evaluated by comparison to the commissioned percent depth dose values using a custom Excel spreadsheet. After determining the uncertainty of the DVH based on these variables,

multiple second check calculations were performed using MIM Maestro and Matlab software packages.

The uncertainties of the DVHs were shown to be less than  $\pm 3\%$ . The average uncertainty was shown to be less than  $\pm 1\%$ . The second check procedures resulted in mean percent differences less than 1% which confirms the accuracy of DVH calculation in Pinnacle and the effectiveness of the quality assurance template.

The importance of knowing the limits of accuracy of the DVHs, which are routinely used to assess the quality of clinical treatment plans, cannot be overestimated. The developed comprehensive QA procedure evaluating the accuracy of the DVH statistical analysis will become a part of our clinical arsenal for periodic tests of the treatment planning system. It will also be performed at the time of commissioning and after any major software/hardware upgrades.

To my astounding wife, amazing parents, and beloved friends, I will never forget the support you have continuously provided me as I take the first steps in achieving my dreams. I love you all forever.

To my Professors, thank you for sharing your knowledge and experience with me. I know that your instruction will guide me as I begin my career and will allow me to make the University of Toledo proud.

## Contents

Abstract.....	iii
Acknowledgements.....	v
Contents.....	vi
List of Tables.....	viii
List of Figures.....	ix
1 Introduction.....	1
2 Motivation.....	10
2.1 ACR Requirements and Recommendations.....	17
2.2 TG-53 Recommendations.....	17
3 Virtual Pinnacle Simulations.....	19
3.1 Dose Volume Histogram Analysis.....	19
3.2 DVH Excel Spreadsheet Calculations.....	24
3.3 Off-axis Evaluation.....	28
3.4 Dose Grid Effect Analysis.....	29
3.5 CT Slice Thickness Effect.....	32
4 Second Check Procedures.....	35
4.1 MIM Second Check Evaluation .....	37
4.2 MATLAB Second Check.....	38
5 Results.....	43
5.1 Dose Volume Histogram Quality Assurance Primary Results .....	43
5.2 Off-axis Evaluation Results.....	48
5.3 Dose Grid Size Evaluation Results.....	52

5.4 CT Slice Thickness Evaluation Results.....	56
5.5 MIM Second Check Results.....	58
5.6 MATLAB Second Check Results.....	60
6 Conclusions.....	64
7 References.....	67
8 Appendix A – DVH to Text Script.....	70
9 Appendix B – Requesting the DVH QA Spreadsheet.....	71



## List of Tables

3.1: Percent Dose Calculation from Dose Volume Histogram QA Spreadsheet.....	25
3.2: Dose to Known Structure Volume from Dose Volume Histogram QA Spreadsheet.....	27
3.3: ROI Dose Calculation from Dose Volume Histogram QA Spreadsheet.....	27
3.4: Cube Contouring and Percent Difference in Pinnacle Volume Estimation Between Plans of Different CT Slice Thickness.....	34
5.1: Dose Volume Histogram Quality Assurance Results.....	43
5.2: Average Percent Differences due to Shifting ROI Structures Off-Axis.....	48
5.3: Average Percent Differences due to Shifting ROI Structures Off-Axis without the Error from Final Dose Bin in DVH Tail Region.....	49
5.4: Primary Dose Grid Evaluation Results.....	52
5.5 Dose Grid Evaluation Results with High Dose Gradient.....	54
5.6: CT Slice Thickness Evaluation Results.....	56
5.7: MIM Second Check Results for Absolute Volume Comparison.....	59
5.8: MIM Second Check Results for Normalized Volume Comparison.....	59
5.9: MATLAB Second Check Results for 2mm Dose Grid Resolution.....	60
5.10: MATLAB Second Check Results for 4mm Dose Grid Resolution.....	62

## List of Figures

1.1: Differential Dose Volume Histogram Sample for a Three-field Pelvis Treatment....	7
1.2: Cumulative Dose Volume Histogram Sample for a Three-field Pelvis Treatment....	8
2.1: Grid Sampling Method Positional Uncertainty.....	11
3.1: ROI Creation Bounding Box with Dimensions.....	21
3.2: 2x2x10 Parallelepiped ROI Structure in Virtual Water Phantom.....	21
3.3: 6x Dose Distribution with Parallelepiped ROI in Virtual Water Phantom.....	23
3.4: Zoomed-in View of Isodose Lines Traversing ROI Structure.....	23
3.5: Setup Image of Dose Grid Evaluation Test in Virtual DVH Phantom with a High Dose Gradient.....	31
3.6: Isodose Distribution of Dose Grid Evaluation Test in Virtual DVH Phantom with a High Dose Gradient.....	32
42.1: View of a Successfully Loaded Plan on CERR.....	41
4.2: Dose Volume Histogram Structure Selection Screen in CERR.....	41
4.3: CERR Generated Dose Volume Histogram.....	42
5.1: Comparison of 6x DVH Dose Results and Calculated Dose Results from Commissioned PDD Data for 2x2x10 ROI Structure.....	44
5.2: Comparison of 10x DVH Dose Results and Calculated Dose Results from Commissioned PDD Data for 2x2x10 ROI Structure.....	45
5.3: Comparison of 18x DVH Dose Results and Calculated Dose Results from Commissioned PDD Data for 2x2x10 ROI Structure.....	45
5.4: Comparison of 6FFF DVH Dose Results and Calculated Dose Results from Commissioned PDD Data for 2x2x10 ROI Structure.....	46

5.5: Comparison of 6x DVH Dose Results and Calculated Dose Results from Commissioned PDD Data for Sphere ROI Structure.....	46
5.6: Comparison of 10x DVH Dose Results and Calculated Dose Results from Commissioned PDD Data for Sphere ROI Structure.....	47
5.7: Comparison of 18x DVH Dose Results and Calculated Dose Results from Commissioned PDD Data for Sphere ROI Structure.....	47
5.8: Dose Volume Histogram for a 6x Beam Exposing the 2x2x10 Parallelepiped at Various Positions Relative to the Central Beam Axis.....	50
5.9: Dose Volume Histogram for a 10x Beam Exposing the 2x2x10 Parallelepiped at Various Positions Relative to the Central Beam Axis.....	50
5.10: Dose Volume Histogram for a 18x Beam Exposing the 2x2x10 Parallelepiped at Various Positions Relative to the Central Beam Axis.....	51
5.11: Dose Volume Histogram for a 6FFF Beam Exposing the 2x2x10 Parallelepiped at Various Positions Relative to the Central Beam Axis.....	51
5.12: Dose Volume Histograms Calculated with Different Dose Grid Resolutions for the Large ROI of 40cm <sup>3</sup> .....	53
5.13: Dose Volume Histograms Calculated with Different Dose Grid Resolutions for the Small ROI of 0.64cm <sup>3</sup> .....	53
5.14: Dose Volume Histograms Calculated with Different Dose Grid Resolutions for a Region of High Dose Gradient to the Large ROI of 40cm <sup>3</sup> .....	55
5.15: Dose Volume Histograms Calculated with Different Dose Grid Resolutions for a Region of High Dose Gradient to the Small ROI of 0.64cm <sup>3</sup> .....	55
5.16: Dose Volume Histogram for Three CT Slice Thickness Settings for 6 MV.....	57
5.17: Dose Volume Histogram for Three CT Slice Thickness Settings for 10 MV.....	57
5.18: Dose Volume Histogram for Three CT Slice Thickness Settings for 18 MV.....	58
5.19: Comparison of 6x DVH Dose Results from Pinnacle and MATLAB with a 4mm Dose Grid in Pinnacle and a 2mm Dose Grid in MATLAB.....	61
5.20: Comparison of 6x DVH Dose Results from Pinnacle and MATLAB with a 4mm Dose Grid in Pinnacle and a 4mm Dose Grid in MATLAB.....	63

## **Chapter 1**

### **Introduction**

As time and technology have progressed so too has the field of radiation therapy. The past one hundred and eighteen years have included a multitude of discoveries, ranging from Becquerel accidentally demonstrating the biological effect of radiation by exposing his chest to radium salt in 1901 to the creation of frameless stereotactic radiation treatment modality. The history of radiation therapy is a testament to the creative prowess of the human condition. The accelerated rate of discovery and development can only be fully understood by separating the timeline into three distinct eras: the Discovery Era began with Röntgen's discovery of X-rays in 1895 and continued into the late 1920's, the Orthovoltage Era continued throughout World War II and ended in 1950 when the Megavoltage Era began. James M. Slater<sup>1</sup> offers a succinct explanation for the rapid advancement of theory and technology throughout the eras, "In each era, the fundamental impetus for improvements came from patients' needs for effective disease control while retaining or improving quality of life<sup>1</sup>." This fundamental drive to continually improve the quality of care provided to cancer patients remains the focus of all research including the development of a quality assurance procedure for dose-volume histogram (DVH) analysis.

The importance of accurately evaluating the effectiveness of a DVH can only be enumerated by briefly examining the history of radiation therapy.

The field of radiation therapy was created on the evening of November 8, 1895 when Wilhelm Röntgen changed the face of human history by discovering the X-ray and igniting the discovery era<sup>2</sup>. Röntgen's newly discovered X-rays were put into use within less than a year in order to treat the first breast cancer patient in 1896<sup>1</sup>. In the same year Becquerel discovered the physical symptoms of radiation exposure and published his report on the phenomenon of radioactivity<sup>1</sup>. Becquerel's discovery was quickly expanded upon by both Marie and Pierre Curie in 1898 and 1901 with the discovery and report on the physical effects of radium. The work of the Curie's spurred the expansion of radium as a new treatment modality in radiation therapy. It wasn't until 1913 that William Coolidge developed the first practical X-ray generating tube. Coolidge's X-ray tube was capable of delivering X-rays of 180 to 200 kV. Physicians were now able to treat tumors at a greater depth within a patient due to higher energy X-rays. The discovery age was defined by theoretical advancements as well as advancements in treatment modalities. Slater summarizes the discovery age by stating, "The discovery of X-rays, then gamma rays, then the structure of the atom with electrons, protons, and neutrons marked the first era<sup>1</sup>."

The orthovoltage era began in the late 1920's and continued until 1950. Throughout this time period the primary method of treatment was the use of radium sources. These sources were generally applied with either intracavitary or interstitial methods in order to apply the necessary dose to the target by placing the source as close

as possible. Brachytherapy with radium sources allowed for simple dose calculation and delivery. It wasn't until 1927 that Rolf Widerøe invented the first linear accelerator by accelerating sodium or potassium ions to 50 keV. Due to the time of his publication, Widerøe's invention was not heavily pursued because nuclear physics research was primarily focused on accelerating lighter particles. It was difficult to accelerate electrons to very high energies at the time because it required much higher frequencies than could be generated in 1927<sup>3</sup>. Due to these setbacks the linear accelerator was not heavily pursued at the time. The cyclotron was conceptualized in 1928 and created in 1930 by Lawrence and Livingston. Robert Van de Graaff created his famous generator in 1929. Donald Kurst developed the Betatron in 1940 which allowed the use of electrons in external beam therapy for the first time with usable energies up to 2 MeV. Throughout this time the second world war had broken out which led to many advances in military technology such as high frequency RF tubes which were implemented as radar detectors<sup>3</sup>. These advancements set the stage for the transition to the megavoltage era and the creation of modern linear accelerators.

The megavoltage era encompasses the greatest period of growth and change in radiation therapy since the discovery of the X-ray. This time period contained the complete replacement of radium as a treatment modality by other elemental isotopes and high voltage external beam treatments. Electron linear accelerators began to become clinically available as early as the mid-1950's with widespread application and implementation in the 1960's and 1970's<sup>1</sup>. New treatment modalities were developed such as cobalt teletherapy machines. 2D simulator machines were created that allowed for more accurate targeting of tumor locations and the development of two-dimensional

treatment plans. As treatment modalities continued to evolve with the usage of higher energy particles treatment planning and evaluation began to face new challenges. One of these difficulties faced by scientists after the development and implementation of high energy linear accelerators was how to control the amount of dose delivered to normal tissues. This struggle led to the development of multi-field treatment plans. The more fields used to treat a target effectively spread the dose to normal tissues over a larger volume thus reducing the extent of the damage but also irradiating more tissue.

Computer-assisted treatment planning began in the late 1990's and led a paradigm shift from 2D planning to 3D planning<sup>1</sup>. The ability to design a treatment plan directly on CT scans drastically increased the achievable accuracy of radiation delivery. The introduction of multileaf collimators, new treatment planning systems, better computer software, intensity modulated radiation therapy, stereotactic radio surgery, volume modulated arc therapy, and other state of the art techniques continue to advance the accuracy of radiation therapy treatments. As planning accuracy increases the importance of minute differences between planned dose distributions from competitive plans also increases. This new era of treatment planning precision created a void for a new evaluation methodology by which modern treatment plans could be compared.

The megavoltage era witnessed the transition from two-dimensional treatment planning to intricate three-dimensional dose distributions to precise targets within patients. The complexity of these treatments often requires a method other than visual interpretation of isodose lines to determine treatment quality. In 1979, Goitein and Verhey introduced the dose-volume histogram, or DVH, as a viable method of evaluating three-dimensional dose distributions as two-dimensional graphs<sup>4</sup>. Upon introduction to

the radiation therapy community the DVH concept floundered for a variety of reasons. In the late 1970's and early 1980's there did not exist enough computer processing power to allow for an accurate dose volume histogram calculation within a reasonable amount of time in a clinic<sup>5</sup>. Only a few institutions even possessed the software necessary for the complex dose calculations. As the years progressed and computer technology became more widely available, the dose-volume histogram became an integral part of three-dimensional treatment plan evaluation in clinics around the world.

Isodose evaluation can often be sufficient for simple plans with a low number of beams however as plan complexity increases so too does the difficulty of comparing multiple plans based solely on isodose lines. The amount of dose information that is displayed on several transverse, sagittal, and coronal planes can be overwhelming. The dose volume histogram offers a simpler evaluation technique by statistical analysis of the dose distribution thus condensing the three-dimensional dose distribution data onto a two-dimensional graph<sup>5</sup>. As a result, DVH's can be used to monitor the dose being delivered to the target volume, healthy tissue, and regions of interest, as well as any hot spots that might arise within the target or in adjacent normal tissues<sup>6</sup>. It is important to note that dose volume histograms contain no positional information. The main utility of the dose volume histogram is a plan evaluation tool.

A dose-volume histogram is created by dividing a volume into a three-dimensional grid of volume elements, known as voxels. The size of the voxel element is small enough such that an assumption can be made that the dose delivered to one voxel is constant within the voxel. The general algorithms used for volume calculation in



treatment planning software are discussed in Chapter 2. The standard voxel size used in TPS at the University of Toledo is 4mm x 4mm x 4mm. This is an adjustable variable that affects the resulting DVH. The impact of this variable on the accuracy of a DVH will be analyzed in this study. In order to evaluate the dose delivered to each voxel a DVH is calculated using bins of equal dose. The volume of interest is divided into dose bins and the voxels are sorted according to their dose bins with no regard for anatomical location<sup>7</sup>. The size of the dose bin is a user adjustable variable and functions as the x-axis of a dose-volume histogram.

A dose-volume histogram is a two-dimensional graph that comes in one of two standard forms: a differential DVH or a cumulative DVH. Differential dose-volume histograms appear as a standard histogram comparing the number of bins receiving the same amount of dose on the x-axis to the volume of the bins on the y-axis. The cumulative DVH plots the dose delivered to the bins versus the relative volume of the critical structures. The cumulative DVH is the standard method of viewing dose-volume histograms because it offers easily interpreted data which a physician can quickly review. Figures 1.1 and 1.2 demonstrate the difference between differential and cumulative dose-volume histograms.

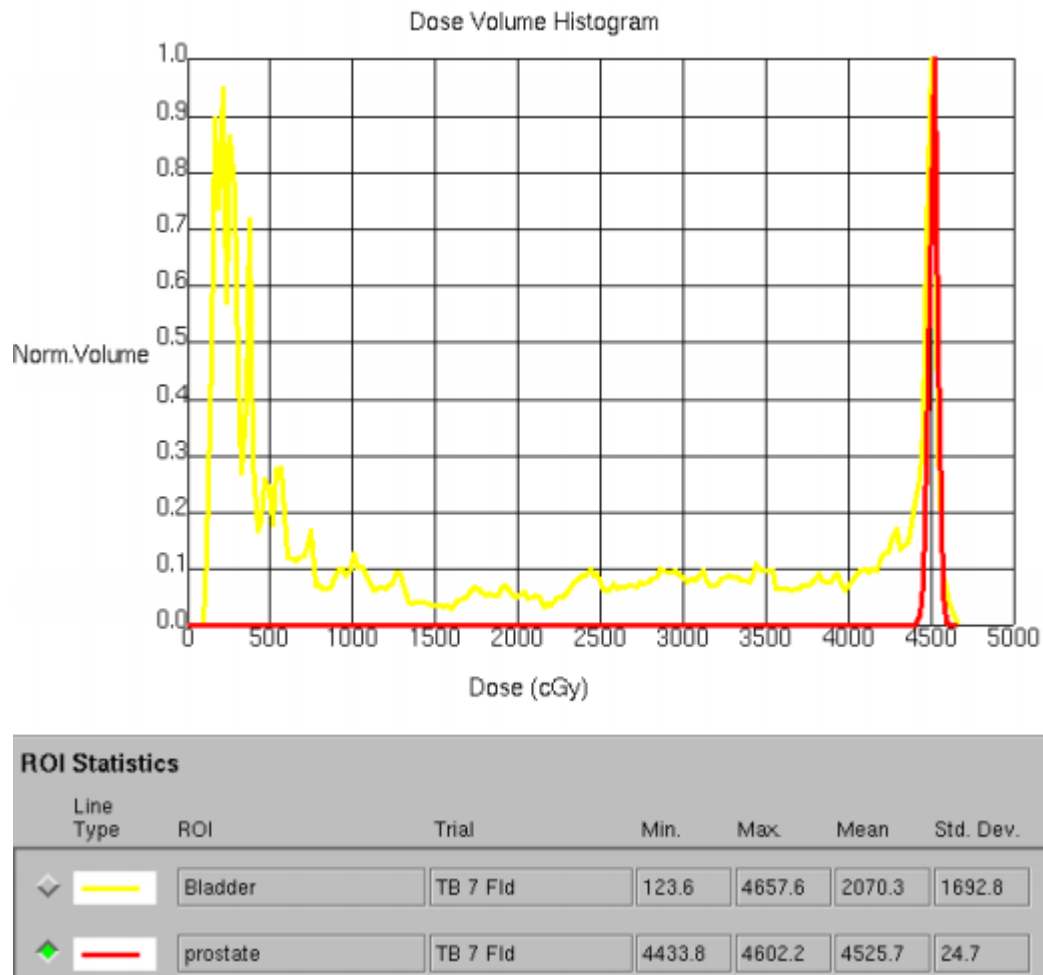


Figure 1.1: Differential Dose Volume Histogram Sample for a Three-field Pelvis Treatment

The differential DVH is necessary in order to accurately compare multiple DVHs calculated with different dose bin sizes. As the dose bin size changes so too does the corresponding amount of volume containing that dose. This change would greatly affect the resultant cumulative DVH however the differential DVH would still allow a direct comparison. If the dose bin widths were increased between two differential DVHs the height of the histogram curves would increase due to more voxels receiving the specified amount of dose however the peaks would still be at the proper locations<sup>8</sup>.

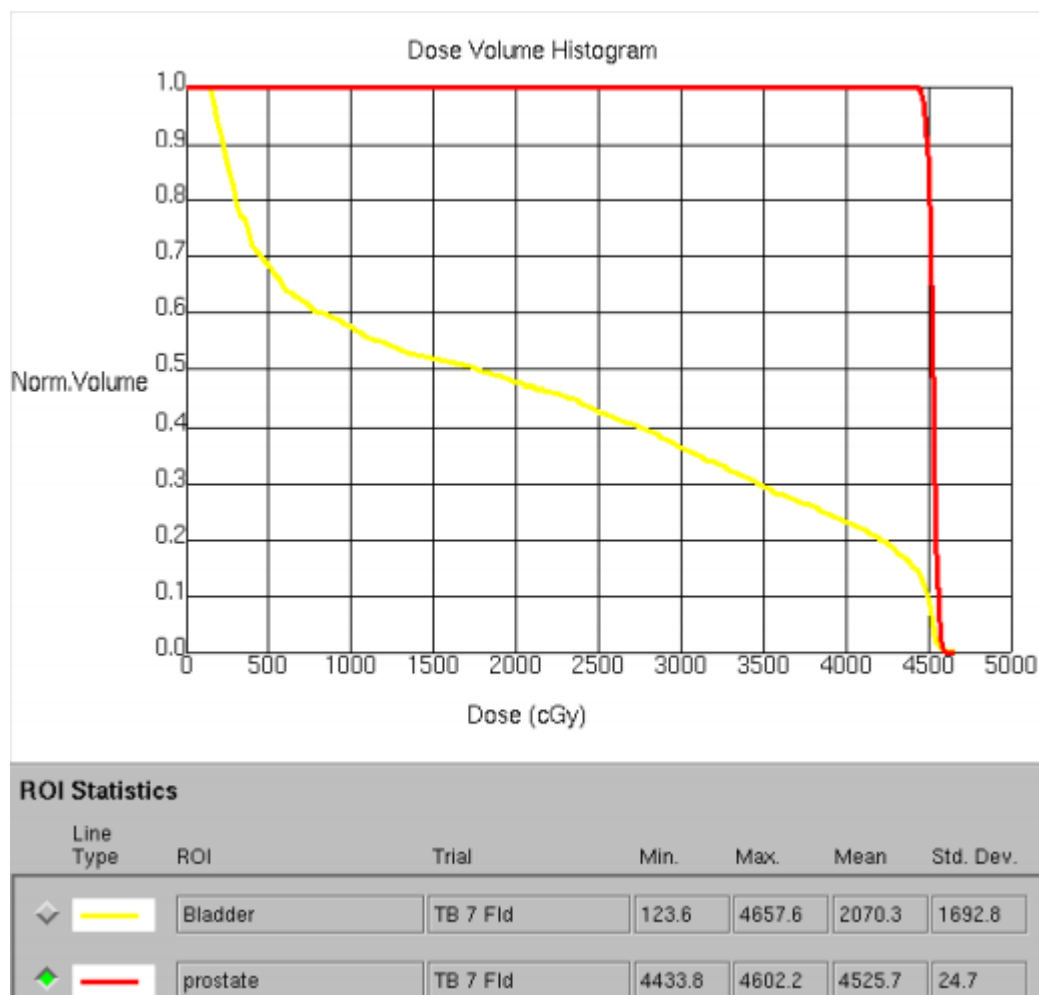


Figure 1.2: Cumulative Dose Volume Histogram Sample for a Three-field Pelvis Treatment

Cumulative dose volume histograms are obtained by adding the volume accumulated in each bin to the volumes in all bins that correspond to higher dose intervals. The cumulative DVH is the standard evaluation tool shown to the physician due to the ease of interpreting dose levels to structures of interest.

Due to the widespread usage of dose volume histograms as an analytical tool to evaluate the quality of a treatment plan, it should be of utmost importance to insure that the data presented on the DVH is accurate to within reasonable tolerances. The

importance of dose volume histograms is only going to increase as further advances in radiation therapy treatment modalities continue to create more complex plans and with the introduction of biologically based treatment planning into the clinical setting. The purpose of this research is to develop a quality assurance procedure for evaluation of the accuracy and uncertainty of dose-volume histograms.

## **Chapter 2**

### **Motivation**

One of the principle responsibilities of a medical physicist is to design and execute quality assurance procedures in order to insure accurate dose delivery. This responsibility carries over into assuring the accuracy of any evaluation tools used in treatment plan evaluation. The importance of the dose volume histogram has only increased with time after its introduction in 1979. Clinicians currently rely heavily on differences shown on dose volume histograms when choosing between competing plans. Due to the clinical importance of dose volume histograms in all aspects of radiation therapy it is imperative that a quality assurance procedure be developed to insure accuracy.

In order to properly evaluate the accuracy of a dose volume histogram a full understanding of DVH calculation techniques is necessary. The name dose volume explicitly states the two important calculations that are required to determine a DVH. The process of dose calculation by dose bins and voxel size has already been addressed. Dose volume histograms are calculated to evaluate the dose given to critical structures and thus the calculation of structure volume is critical in the accuracy of the DVH. There exist two

standard methods for volume calculation methods: grid-based sampling and random sampling<sup>9</sup>.

The original volume calculation technique for determining dose volume histograms was the grid sampling method. The grid sampling method is designed by superimposing a grid of evenly spaced points over the entirety of the CT scan. The volume of a structure is determined by the number of points residing inside the structure. The separation between the points of the grid is constant and thus by knowing the number of points within the structure of interest the volume of the structure can be calculated. This calculation suffers from some inherent uncertainties when calculating ROI volumes. Figure 2.1 demonstrates how the grid sampling method can suffer from uncertainty when calculating the volume of three objects based solely on their relative position on the grid.

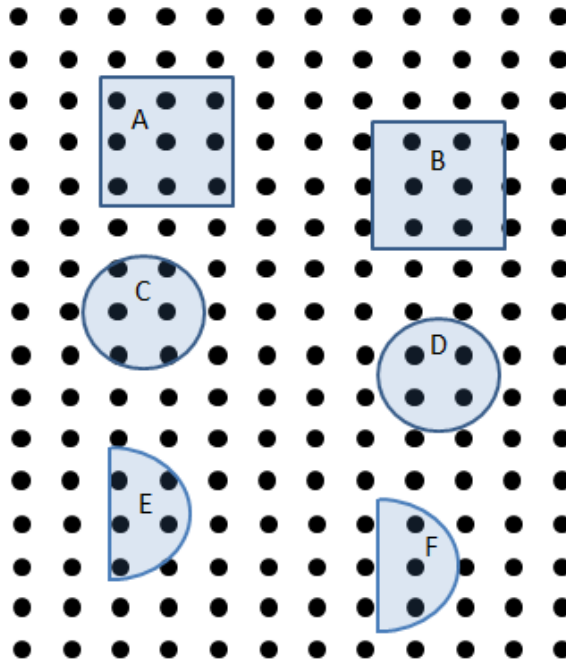


Figure 2.1: Grid Sampling Method Positional Uncertainty

Figures A and B, C and D, E and F all have the same volume respectively and represent voxel elements. The two-dimensional area of an ROI is determined by the number of grid points residing inside the ROI. In Figure 2.1 the area of object A would be calculated by the nine points within the object. Object A would have an area of  $4t^2$  where  $t$  is the distance between grid points. Object B has the same physical area of object A however it only contains six points and would result in an estimated area of  $2t^2$ . Similar errors occur for objects C and D and objects E and F. This example clearly demonstrates that the estimation of area, or volume for a three-dimensional voxel, depends on the registration between the structure of interest and the calculation grid. Niemierko et al. demonstrates that the average absolute value of the relative error of volume estimation for a cubic ROI can be approximated by the following equation<sup>9</sup>.

$$\delta_{grid}^{volume} = \frac{\Delta V}{V} = \frac{1.5}{N^{1/3}} \quad (2.1)$$

$V$  is the structure volume and  $N$  is the number of grid points lying within the volume.

Equation 2.1 can be rewritten as a function of grid size and structure volume.

$$\delta_{grid}^{volume} = \frac{1.5t}{V^{1/3}} \quad (2.2)$$

These two formulas were calculated for a cubic region of interest however based on the example of Figure 2.1 a similar relationship exists between the relative errors of the grid sampling method for other shapes.

The second method used to calculate a structure's volume is random sampling. The random sampling method consists of setting a parallelepiped of dimensions around the structure of interest that is large enough to cover the entire structure. Once this is

completed the calculation selects points randomly within this parallelepiped. If a number of points,  $N_0$ , have been selected with a uniform probability density function within a known volume,  $V_0$ , then each point represents an elementary volume defined by

$$\Delta V = \frac{V_0}{N_0} \quad (2.3)$$

where  $V_0$  is the total volume of the parallelepiped surrounding the structure<sup>6</sup>. If among these  $N_0$  points,  $N'$  points have been found within the structure, the volume of the structure may be approximated by  $N' \cdot \Delta V$ . A dose volume histogram can be obtained and plotted by calculating the dose at each of these  $N'$  points. A more accurate calculation of the unknown volume can be achieved by applying the basic Monte Carlo integration theorem.

$$V = V_0 \frac{N'}{N_0} \pm V_0 \sqrt{\frac{\frac{N'}{N_0} - \left(\frac{N'}{N_0}\right)^2}{N_0}} \quad (2.4)$$

Niemierko et al. demonstrate that the relative error for this volume estimation calculation technique is

$$\frac{\Delta V}{V} = \frac{V_0}{V} \sqrt{\frac{\frac{N'}{N_0} - \left(\frac{N'}{N_0}\right)^2}{N_0}} = \frac{1}{\sqrt{N_0}} \sqrt{\frac{N'}{N_0} - 1} = \frac{1}{\sqrt{N_0}} \sqrt{\frac{V}{V_0} - 1} \quad (2.5)$$

where  $\frac{V}{V_0}$  reduces to 2 for the smallest cubic shaped reference volume which simplifies the relative error of the random sampling method to the following equation<sup>9</sup>.

$$\delta_{random}^{volume} = \frac{1}{\sqrt{N_0}} \quad (2.6)$$



Now that the relative error has been determined for both volume calculation methods the quality of each can be compared. By evaluating equations 2.2 and 2.6 it is clear that the random sampling calculation requires far fewer sampling points in order to achieve a given accuracy.

DVH's often differ in complex and varied ways and the implications of those differences are not always clear. The effect of a small change in the value of one bin of a histogram depends on the circumstances. For example, a slight reduction from 100% volume in the lowest dose bin could have a large impact on tumor control however it would have negligible consequences for normal tissue response<sup>9</sup>. One common complication that arises from the grid sampling method involves using different grid sizes for dose computation and for DVH calculation. In order to increase calculation speed, many sites use a coarse grid for dose computation and then interpolate into a finer grid for DVH analysis. The smaller spacing provides greater accuracy for volume estimates. This issue will be addressed later in this paper. In order to fully understand the impact of sampling method selection, Niemierko et al. suggests that the best evaluation parameter of DVH quality is to analyze the biological implications of the resultant histogram<sup>9</sup>.

The future importance of biologically based treatment plan evaluation is one of the major motivations for developing DVH quality assurance procedures. Tumor control probability, TCP, is calculated directly from a dose volume histogram. A simplistic version of the TCP model involves partitioning the tumor into sub-volumes known as tumorlets. The dose within each tumorlet is essentially uniform. When computing TCP

from a DVH the tumorlet has a one-to-one correspondence with the bins of the DVH. The tumor control probability can be calculated by the following equation

$$TCP = \prod_{i=1}^M [TCP(D_i)]^{v_i} \quad (2.7)$$

Where M is the number of subvolumes, or bins, in the DVH of the partial volume  $v_i$  and average dose to the subvolume  $D_i$ <sup>9</sup>. Normal tissue complication probability, NTCP, is calculated in a similar fashion and the relative errors for both are determined in a similar manor as the previous volume calculations. Thus for a given formulation of a biological end-point and a given number of calculation points, N,

$$\frac{\delta_{grid}^{TCP}}{\delta_{random}^{TCP}} = \frac{\delta_{grid}^{NTCP}}{\delta_{random}^{NTCP}} = \frac{\delta_{grid}^{volume}}{\delta_{random}^{volume}} = \frac{\frac{1.5}{N^{1/3}}}{\frac{1}{N^{1/2}}} = 1.5N^{\frac{1}{6}} \quad (2.8)$$

This equation simplifies the determination of the number of grid points required for the grid sampling technique to achieve the same accuracy as randomly generated points<sup>9</sup>.

$$N_{grid} \cong 3.4N_{random}^{3/2} \quad (2.9)$$

This conclusion demonstrates that the random sampling method of volume calculation is always more accurate than a grid sampling method for the same number of points.

Utilizing the random sampling method for volume calculation allows for less inherent uncertainty in dose volume histogram calculation while increasing the overall speed.

The random sampling method offers the greatest accuracy for volume estimation in dose volume histogram calculation however there remain situations that could induce error in the DVH. A relevant example of this occurs when calculating the volume of an irregularly shaped object on a patient's CT. If the dose grid is not sufficiently small, for

the grid sampling method, or there are not enough randomly generated points, for random sampling, it is easy for a volume calculation to miss cold spots. These errors are easily kept to a minimal level by increasing the number of randomly selected points for the random sampling method. The only drawback of increasing the number of points is a reduction in calculation speed so this procedure need not be utilized unless a volume of interest is obviously a candidate for irregular shaped extremities which may suffer from a cold spot.

Other situations that can induce error in the dose volume histogram calculation include comparisons of separate plans. When comparing plans that were computed using different dose computation parameters or different dose calculation algorithms there are always some uncertainties in dose volume histogram calculation and representation. This effect is primarily a concern when receiving copies of a patient's past treatment from a different institution that uses different planning software. The uncertainty in the DVH calculation between these plans stems from different dose algorithms measuring tissue heterogeneities or beam penumbra in different ways. Changes in sampling techniques and dose bin settings can also have an effect between DVHs.

Some uncertainties in dose volume histogram calculation are caused by different voxels experiencing different irradiation conditions. Different voxels that measure the same absorbed dose can be exposed to very different irradiation conditions such as penumbra, high dose gradient, proximity to high or low density organs, or under a beam modifier such as a multileaf collimator for a control point<sup>10</sup>. Care must be taken when

planning in order to avoid some of these situations and insure more accurate dose volume histogram results.

## **2.1 ACR Requirements and Recommendations**

The American College of Radiology publishes standards and recommendations that must be met by active medical physics radiation oncology departments when they chose to seek accreditation by the ACR. According to the Technical Standard for the Performance of Radiation Oncology Physics for External Beam Therapy, revised 2010, “If dose-volume histograms are used in the analysis of the plan, their validity must be checked. Various dose distributions can be calculated whose characteristics are known. The dose and volume results from the dose-volume histogram can be checked against the known values<sup>11</sup>.” This requirement was re-iterated in the ACR-ASTRO Practice Guideline for 3D External Beam Radiation Planning and Conformal Therapy, revised 2011, which stated that a physicist must confirm the accuracy of the system-generated dose volume histograms or other “tools” or reports used for plan evaluation<sup>12</sup>.

## **2.2 TG-53 Recommendations**

The American Association of Physicists in Medicine published dose volume histogram quality assurance recommendations in Task Group 53. The AAPM recommends that DVH calculation and output be evaluated for accuracy<sup>13</sup>. TG 53 does not state a tolerance value for DVH quality assurance but explains that this value depends on many different elements as outlined previously.

## **Chapter 3**

### **Virtual Pinnacle Simulations**

An important aspect of all quality assurance procedures is ease of reproducibility. A well designed quality assurance procedure will be applicable to any similar machine and will allow for simple evaluation of important clinical aspects of treatment. This chapter describes the process used to create a virtual phantom of known volume in order to evaluate the accuracy of dose-volume histograms. Any user will be able to easily recreate the setup for this experiment by following the described procedure. This will assure a reproducible and accurate quality assurance test.

#### **3.1 Dose Volume Histogram Analysis**

The basis for this procedure was outlined by Gossman in his paper, “Dose-volume histogram quality assurance for linac-based treatment planning systems<sup>14</sup>.” The following instructions have been modified to better suit the needs of this experiment and to allow

for better reproducibility. A new patient was first created in Philips Pinnacle (Andover, USA) under the name Virtual DVH Phantom. This experiment was designed to be entirely virtual and thus there is no need to import any treatment planning images. Pinnacle has the option of loading virtual phantoms and a 50x50x50 cm<sup>3</sup> water tank was selected for this patient. This virtual water tank permits for large field size beams, such as 30x30 cm<sup>2</sup>, while allowing enough extra space in order to avoid dose variations at the sides of the tank. The next step of this procedure was creating the known volume.

A known volume with easily measured dose distribution is necessary for DVH evaluation. A parallelepiped was selected for this reason. By evaluating a volume of a known height, width, and length, it is possible to calculate the expected amount of dose that should be delivered to that volume based on commissioned depth dose measurements for the linear accelerator. The volume was created such that it was 2 cm wide and 2 cm in length that extended for a height of 10cm. Thus the theoretical volume of the created parallelepiped should be 40 cm<sup>3</sup>. In order to avoid scatter from the surface, the parallelepiped was placed such that the top of the volume was at a depth of 5 cm with the bottom at 15 cm. In order to create this volume in Pinnacle it was necessary to utilize the auto contouring options. It would be extremely difficult to input this contour by hand with any semblance of accuracy and thus a bounding box was created at the coordinates described above. The exact input of the bounding box is given in the following figure.

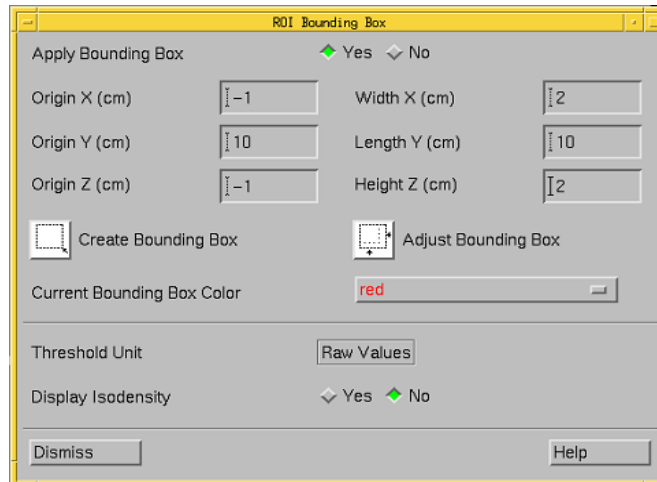


Figure 3.1: ROI Creation Bounding Box with Dimensions

After the bounding box was created at the proper position in the water phantom, the parallelepiped was contoured using the auto contouring tool that creates a structure based on Hounsfield unit parameters that are restricted by the bounding box.

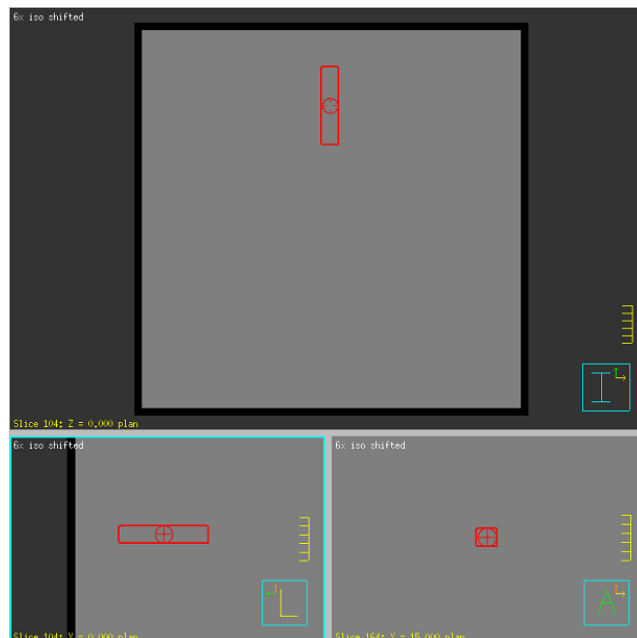


Figure 3.2: 2x2x10 Parallelepiped ROI Structure in Virtual Water Phantom



The created structure has one extra slice due to the auto contouring tool in Pinnacle however this was easily resolved by selecting one of the outermost contours and deleting it. After correcting for this extra slice the contour should have 8 sagittal slices 0.250 cm thick giving it a 2 cm width. Pinnacle calculated that the resulting structure had a volume of  $40.125 \text{ cm}^3$ . This is less than 0.4% different from the ideal volume of  $40 \text{ cm}^3$  and will allow for accurate dose evaluation. An isocenter was placed at the center of the parallelepiped at 10cm depth. A beam was created with a field size of  $30 \times 30 \text{ cm}^2$  centered at the isocenter. A prescription was created to deliver 100 cGy to the isocenter. This trial was copied multiple times in order to set the beam to different energies for evaluation.

Once the known volume was successfully created, the dose was computed and the dose-volume histogram could be evaluated. The parallelepiped was chosen because it was easy to delineate the amount of dose given to precise volumes due to the flatness of the dose profile. 100 cGy was delivered to the isocenter at a 10 cm depth; since the dose profile at this depth near the central axis is almost perfectly flat, the 100 percent isodose line crosses the parallelepiped at 10 cm depth. This is shown in the following Figures 3.3 and 3.4.

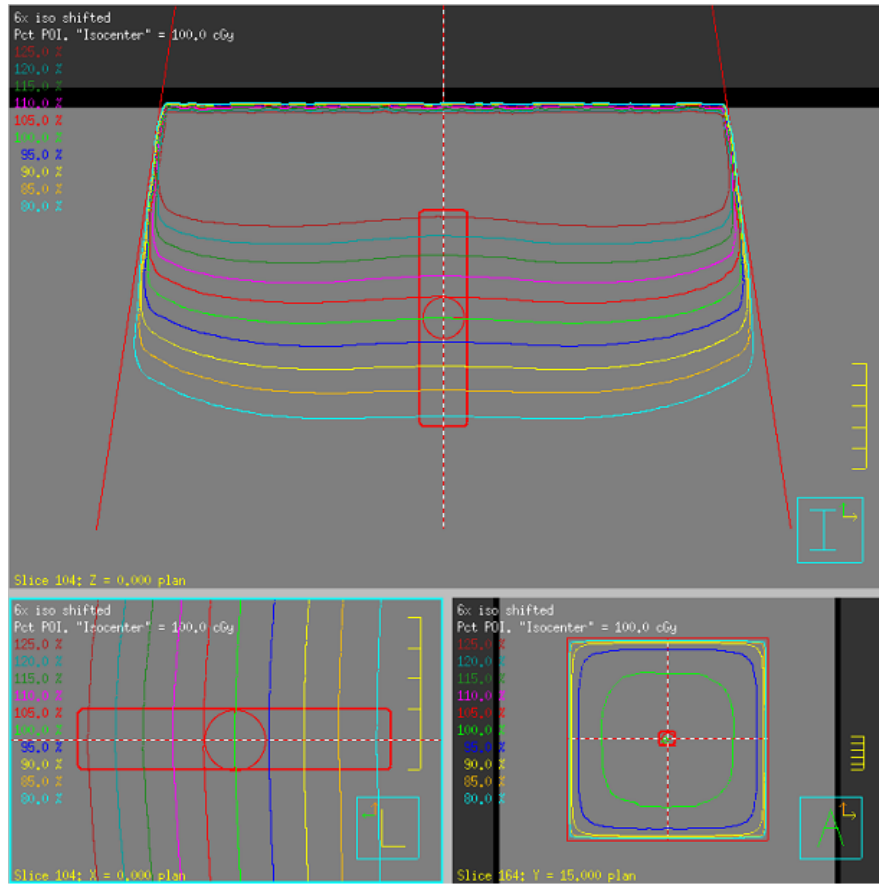


Figure 3.3: 6x Dose Distribution with Parallelepiped ROI in Virtual Water Phantom

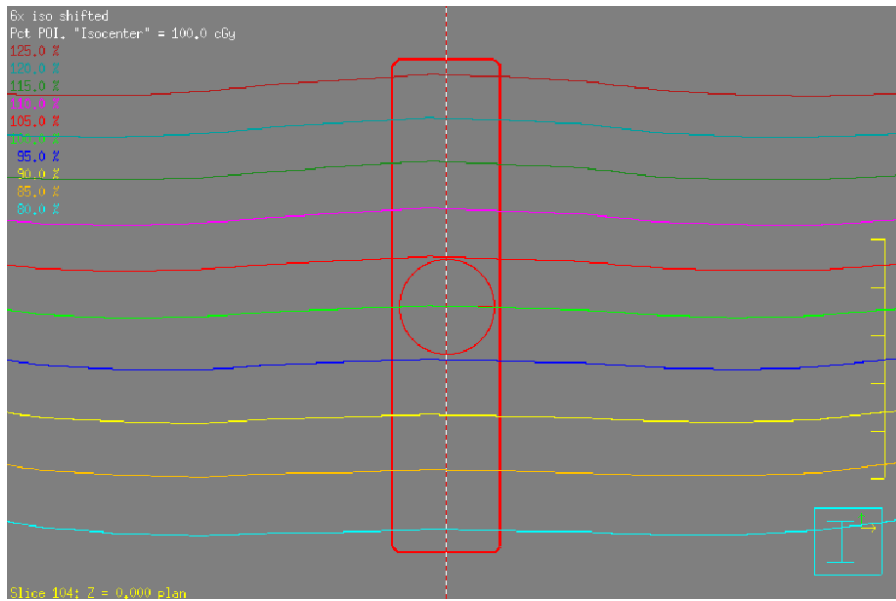


Figure 3.4: Zoomed-in View of Isodose Lines Traversing ROI Structure

This feature allows for a direct comparison between expected theoretical values which are determined using the commissioned data from the machine and the measured dose-volume histogram results.

### **3.2 DVH Excel Spreadsheet Calculations**

Pinnacle allows the user to view the numerical data of each DVH. This information is referred to as a tabular DVH and is quintessential for this study. The tabular DVH information was evaluated in order to determine the amount of dose delivered to a specific volume of the structure. This evaluation was accomplished by creating a Microsoft Excel workbook template that takes the text file output of the tabular DVH and analyzes the information. A script was used to obtain a text file of the tabular DVH. The procedure for executing the script is given in Appendix B. The printing script was modified from a base script which was obtained from a public access medical physics database<sup>15</sup>. The script was changed so that the printed DVH data would be printed in 1cGy dose bins and exported to a custom location. This script copies the information from the tabular DVH and prints a text file that includes dose values and the volume of the structure receiving that dose. This text file was then opened in Excel and copied into the template.

The template is designed to facilitate evaluation of the accuracy of computed dose-volume histograms. In order to use the template one must have the commissioned output and percent depth dose curves for the specific treatment machine. Using the percent depth dose values at varying depths allows for the calculation of percent dose delivered to a known percentage of the structure volume. This is done by normalizing the percent dose delivered to the isocenter at 10 cm depth to equal exactly 100% of the prescription, 100 cGy. This is shown in the following table for 6 MV x-ray beam. The normalization factor was found using equation 3.1.

$$\%DD \text{ to } \%Dose \text{ Normalization Factor} = \frac{100}{\%DD \text{ at } 10cm} \quad (3.1)$$

The commissioned percent depth dose values are then multiplied by this normalization factor to result in the expected percent dose values.

Table 3.1: Percent Dose Calculation from Dose Volume Histogram QA Spreadsheet

Energy	Depth (cm)	% Volume	%DD (commissioned)	% D (at d) Calc
6 MV	6	10	84.49	118.98
	7	20	80.92	113.96
	8	30	77.53	109.18
	9	40	74.25	104.56
	10	50	71.01	100.00
	11	60	67.95	95.69
	12	70	64.86	91.34
	13	80	62.05	87.38
	14	90	59.26	83.45
	15	100	56.48	79.54

These percent dose values will be used to evaluate the accuracy of the dose-volume histogram percent dose output.

Once the DVH output script file has been put in the template, the measured dose to specific volumes will be determined for each energy. This procedure requires some interpolation due to the nature of Pinnacle's tabular DVH formatting. The smallest bin size is set to 1 cGy and thus it is not possible to obtain the exact dose to a specific volume without some interpolation. The following example is using the DVH output data for the 6 MV beam. In order to calculate the dose delivered to 20 cm<sup>3</sup>, or the central axis of the structure, the spreadsheet will determine the difference factor between the two volumes surrounding the desired volume and multiply this value by 100. Due to the dose bin size being 1 cGy the difference between these volumes is always going to be 1 cGy. The spreadsheet then calculates an interpolation factor that is 1 cGy divided by the difference factor defined below. The dose is then determined by adding the dose to the volume greater than the target volume with the interpolation factor multiplied by the difference of the volume greater than the target and the target volume. This calculation is shown in the following equations:

$$Difference\ Factor = (Vol_{>Target} - Vol_{<Target}) * 100 \quad (3.2)$$

$$Interpolation\ Factor = \frac{1\ cGy}{Difference\ Factor} \quad (3.3)$$

$$Dose = Dose_{Vol>Target} + [Interpolation\ Factor * 100 * (Vol_{<Target} - Vol_{Target})] \quad (3.4)$$

The following Table 3.2 is an excerpt from the spreadsheet showing these equations in use.

Table 3.2: Dose to Known Structure Volume from Dose Volume Histogram QA Spreadsheet

Corrected Dose (cGy)	Volume (cm <sup>3</sup> )	depth	difference * 100	1cGy/dif*100	dose to 20cm^3
100	20.5	10	77	0.013	100.65
101	19.73				

The spreadsheet applies this method to every beam energy for the known volume

exposed at each depth from 6cm to 15cm in 1 cm intervals as shown in Table 3.3.

Table 3.3: ROI Dose Calculation from Dose Volume Histogram QA Spreadsheet

Depth (cm)	ROI Height (cm)	Target Vol (cm3)	6x Dose (cGy)	10x Dose (cGy)	18x Dose (cGy)	6fff Dose (cGy)
5	0	0	127.37	124.06	120.77	131.11
6	1	4	121.62	118.92	117.30	124.63
7	2	8	116.44	113.73	112.92	117.54
8	3	12	111.22	109.25	108.63	111.73
9	4	16	106.05	104.93	104.62	106.10
10	5	20	100.65	100.60	100.60	100.26
11	6	24	95.64	96.41	96.64	94.79
12	7	28	91.24	92.38	92.97	89.84
13	8	32	86.90	88.49	89.43	84.93
14	9	36	82.67	84.71	85.98	80.28
15	10	40	78.51	81.07	82.61	75.79

Now that the spreadsheet has the precise dose delivered to the specific target volume at each depth it is possible to calculate the accuracy of the dose volume histogram.

The percent difference between the dose-volume histogram data and the commissioned percent dose values can now be determined. Using this value it is simple to calculate the percent difference between the DVH and the expected dose to this volume.

$$DVH \% Difference = \left| 1 - Dose \left( \frac{Calculated}{DVH} \right) \right| * 100 \quad (3.5)$$

### 3.3 Off-axis Evaluation

When a patient is exposed to radiation therapy, the act of breathing induces organ motion. For some patients this is a large enough concern to warrant additional techniques to limit the influence of respiratory motion such as gating and compression. For most patients however they are told to breathe normally. This motion is generally not significant enough to cause any worry for OAR and it compensated for targeted treatments by the physician-drawn PTV which overestimates the size of the tumor in order to account for organ motion. An off-axis evaluation test was included in this quality assurance procedure in order to evaluate the effect of an organ shifting in a uniform homogenous phantom. This is an oversimplified test which does not correlate to every situation in the human body due to regions of different tissue heterogeneities. This test does serve as an evaluation of the impact of the position of an ROI with respect to the dose grid as well as beam flatness and symmetry using the dose volume histogram calculation.

This test was performed by evaluating the effect of shifting the region of interest off axis by a known distance. The previously described  $40\text{cm}^3$  parallelepiped was recreated at three different positions within the virtual DVH water phantom. A new ROI was created with identical dimensions at positions located 0.5cm, 1.0cm, and 1.5cm offset from the central axis. These shifts were used in order to simplify the creation of the ROI structure while shifting the structure within the size of a voxel. The dose grid is

4mm and thus the 0.5cm shift is a shift of one voxel and 1mm, the 1.0cm shift is two voxels and 2mm, and the 1.5cm shift is three voxels and 3mm. This allowed for the effect of slight shifts within a voxel to be quantified by shifting the ROI a known value in reference to the stationary dose grid within the spacing of one voxel. The resulting dose volume histograms were exported using the printing script and evaluated by the quality assurance spreadsheet. The values of maximum, minimum, and mean doses were also input into the spreadsheet. The results of this test are given in the Chapter 5.

### **3.4 Dose Grid Effect Analysis**

The tests described in this section were performed in order to ascertain the effects of adjusting the dose grid resolution in Pinnacle on calculated dose volume histograms. The effect of adjusting the dose grid resolution should alter the DVH calculation of a small volume of interest greater than that of a larger volume of interest. A smaller volume of interest will experience greater differentiation in segmentation by different size dose grids which could increase the induced uncertainty when adjusting the resolution. A new ROI structure was created with a smaller volume of  $0.64\text{cm}^3$  in order to compare the effects of changing the dose grid between the large volume of the  $2\times 2\times 10\text{ cm}^3$  parallelepiped,  $40\text{cm}^3$ , and the smaller volume parallelepiped with dimensions  $0.25\times 0.25\times 10\text{ cm}^3$ . The Virtual DVH Phantom was evaluated for 2mm, 3mm, 4mm, and 5mm dose grids. A 4mm dose grid is the standard for the University of Toledo and was used as the standard result by which the other dose grids were analyzed in order to



determine the induced percentage difference between the dose grid resolutions. Two separate tests were executed so that the dose grid resolution could be evaluated for different conditions. The first test utilized the same conditions as the primary DVH analysis only changing the dose grid resolution. The second test was designed in order to test the effect of adjusting the dose grid resolution in a region of high dose gradient.

For the first test, the only variable changed between each plan was the dose grid. The dose distribution for the Virtual DVH Phantom is very homogenous and thus the expected result of changing the dose grid was that there should not be a drastic difference induced in the DVH results. The second test required the introduction of a high dose gradient region. The original plan was copied and a new beam was added to each trial. This beam was set to a gantry angle of 10 degrees with an adjusted field width in the x-axis such that the beam would pass through the ROIs without fully covering the ROI. The prescription of this beam was set to deliver 15cGy to the isocenter. This setup would induce regions of high dose gradient throughout the entire volume. Figure 3.5 shows the two beam setup for this test.

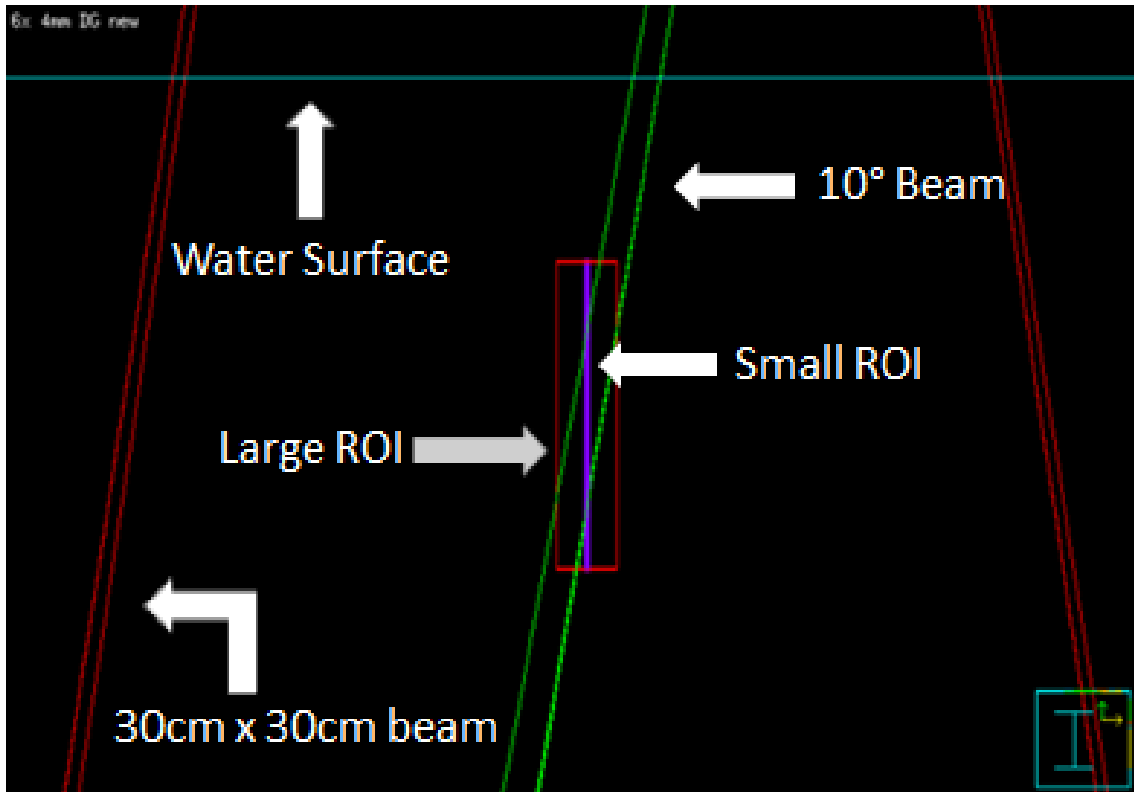


Figure 3.5: Setup Image of Dose Grid Evaluation Test in Virtual DVH Phantom with a High Dose Gradient

The resulting isodose distribution shown in Figure 3.6 clearly shows the regions of high dose gradient throughout the ROIs.

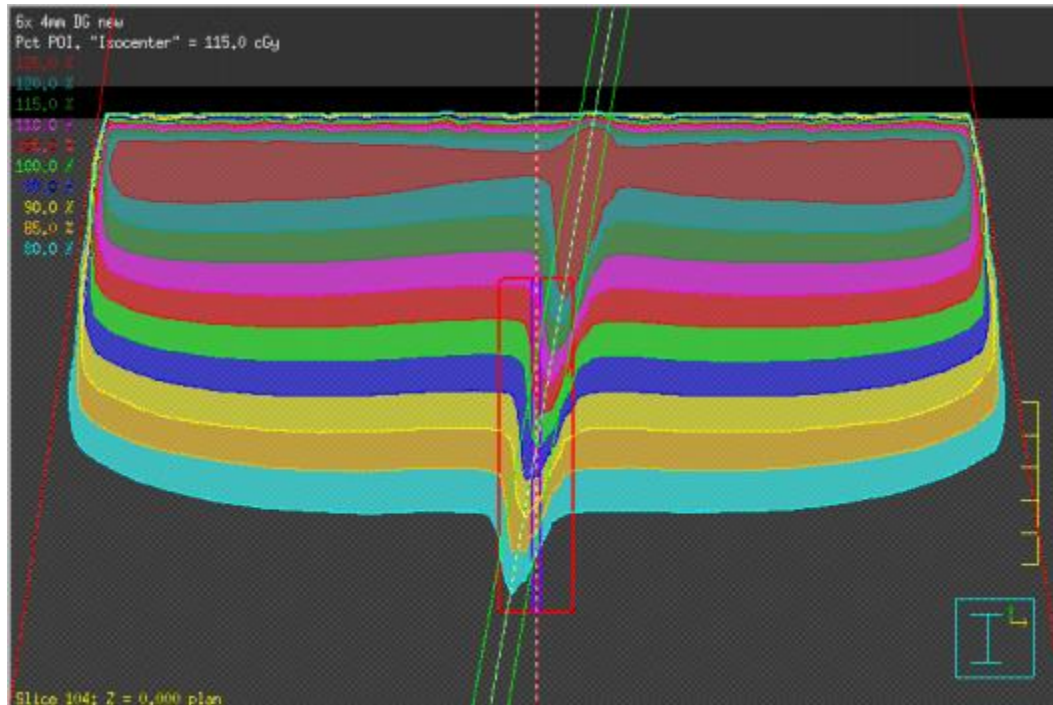


Figure 3.6: Isodose Distribution of Dose Grid Evaluation Test in Virtual DVH Phantom with a High Dose Gradient

Two separate tests of the dose grid effect were performed. The initial test without the high dose gradient was done with the same method as the primary DVH evaluation. Due to the influence of the second beam the evaluation of the high dose gradient region had to be modified, since it was not possible to determine the exact dose to known depths without inducing calculation errors. Therefore in the latter test, a direct evaluation of the resulting normalized volume found for a chosen dose bin and comparing the normalized volume with that of the 4mm grid size value was performed. The results of both tests are enumerated in Chapter 5.

### 3.5 CT Slice Thickness Effect

One of the important user-specified parameters that is set when a patient receives the required treatment planning CT is the width of the CT slice thickness spacing. Most institutions have a standard slice thickness for various scan types. For procedures requiring a greater level of precision smaller slice thicknesses can be chosen. This is often done for small tumors in head and neck cancers. The standard setting for a body scan at the University of Toledo is 3mm. The initial selection does not inherently create uncertainty in dose calculations in Pinnacle. Uncertainties can become relevant when comparing a plan between two different CTs with different slice thicknesses. The amount of uncertainty inherent for this situation was determined by comparing three identical plans across three slice thickness settings for the same CT scan.

A 5x5x5 cm<sup>3</sup> plastic cube was scanned using a Phillips Gemini TF Big Bore PET/CT scanner. The cube was placed on a base so that the bottom of the cube could be easily differentiated on the CT for simpler contouring in Pinnacle. The CT was taken with the standard brain protocol. The resulting CT was then reconstructed with different slice thickness settings. The CT was exported with three different scans of 0.75mm, 1.5mm, and 3.0mm slice thicknesses for evaluation in Pinnacle. The couch position was located with the 0.75mm-slice CT at -14.63cm and removed in all three plans at the same value for consistency. The same procedure was used to determine the isocenter of the 0.75mm-slice CT. The center of the cube was determined from the transverse, longitudinal, and axial views of the CT. The isocenter was set to the same position on all three plans. The cube was contoured on each plan using a bounding box to eliminate the base from the contour.

Table 3.4: Cube Contouring and Percent Difference in Pinnacle Volume Estimation Between Plans of Different CT Slice Thickness

CT Slice Thickness	Volume (cm <sup>3</sup> )	% Difference
0.75 mm	125.008	0.0064
1.5 mm	125.001	0.0008
3.0 mm	125.012	0.0096
Ideal	125	

Table 3.4 shows that the contours of the cube will not contribute any significant error when comparing the results of the dose volume histograms for the three plans. Each contour was calculated by Pinnacle to be less than 0.01% different than the actual volume of the cube.

After contouring the cube was completed, a new ROI was created by expanding the cube in all directions except anteriorly by 4cm. This new contour was named water + 4cm expanded cube and overridden to the density of water. This step was to eliminate the influence of a small metal ball at the center of the cube phantom and any influence of wall scatter within the cube itself on the dose calculation, thus insuring similar irradiation conditions for the three different plans. Each plan contained three trials for each energy evaluated, 6, 10, and 18 MV. Each beam was identical and set to the isocenter for the same prescription. The tabular dose volume histogram data was exported using the script and evaluated in the quality assurance spreadsheet.

## Chapter 4

### Second Check Procedures

In order to develop a versatile quality assurance procedure it is necessary to create some redundancies so that the user will not receive false passing rates. This was achieved utilizing two different second check procedures. The first evaluation technique utilizes MIM Maestro 5.6.5 and the second method involved MATLAB<sup>16,17</sup>. Both methods involved exporting a DICOM file of the DVH test plan to the separate programs to create dose volume histograms with different calculation algorithms than Pinnacle. If the dose volume histogram created by the secondary check technique for the same plan is very similar to the Pinnacle DVH the results of the Pinnacle evaluation are confirmed. When following this quality assurance procedure it is unnecessary to perform a second check evaluation with both MIM and MATLAB. If the QA results are confirmed with one second check procedure, there is no need for a third check.

The first step in creating both second check techniques was to export the DVH evaluation plan and dose to a DICOM file. For ease of use and reproducibility, the DVH evaluation plan was recreated on the CT scan used for CT slice thickness evaluation. The plan had to be adjusted to meet the constraints of the CT size and width. The new field size was adjusted to 20 x 20 cm<sup>2</sup> instead of 30 x 30 cm<sup>2</sup>. This reduction should not have an effect on the measured dose distribution or DVH calculation because there is still a large enough gap between the beam divergence and any sources of scatter. A region of

interest was contoured on the CT such that it was the same size as the desired water phantom. In order to fully recreate a virtual water phantom on a CT scan of another object this structure was density overridden to have the density of water for all dose calculations. Once an effective, if smaller, water tank was simulated on the CT, the DVH evaluation plan was recreated using the same procedure as previously described.

After recreating the original DVH evaluation plan on the new CT-based plan there was a new opportunity to study the DVH accuracy with a different volume of interest. One advantage of the CT based plan was that it became possible to export the plan to MIM, create a spherical volume structure of known volume, and import the new structure into Pinnacle for evaluation. Initially there were three spherical structures created of various diameters: 42mm, 43mm, and 44mm. These structures were evaluated after being imported into Pinnacle and the sphere with the closest volume to  $40\text{cm}^3$  was chosen, 42mm. This size of sphere was created to have a direct comparison volumetrically between the parallelepiped and the sphere. The inclusion of a spherical structure as an evaluation tool is to quantify any inherent errors in Pinnacle dose volume histogram calculation caused by the interpolation of dose data in corners, as described by Veld et al.<sup>18</sup> The sphere was centered at the isocenter with a depth of 10 cm on the same axis as the parallelepiped. After importing the structure into Pinnacle the radius of the sphere was measured to be 2.12cm resulting in a volume of  $39.8\text{cm}^3$ . For the evaluation of the calculated dose at depth for the DVH versus the commissioned percent depth dose values it was necessary to calculate the volume of the sphere at different depths. This was accomplished by applying the following formulas:

$$\text{Offset Radius } (c) = \sqrt{h(2r - h)} \quad (4.1)$$

$$\text{Partial Volume of Sphere} = \frac{\pi}{6}h(3c^2 + h^2) \quad (4.2)$$

Where h is the portion of the sphere from the tip to the depth of evaluation and r is the radius. Utilizing this information the spreadsheet was able to evaluate DVH accuracy for both the parallelepiped structure and the spherical structure.

#### **4.1 MIM Second Check Evaluation**

Once the DVH evaluation plan was updated to include the spherical volume it was exported to MIM. Each energy was evaluated in a different trial and each trial was exported separately. The DICOM files were accessed in MIM and the plan and structures were selected and opened in a new session. The dose for each trial was loaded individually to create a DVH. The resulting DVH calculated in MIM was saved as a .csv file which can be opened and evaluated in Excel. The .csv file from MIM lists the tabular information in 1cGy increments with the volume of each structure receiving that amount of dose. These files should be saved with a well-chosen name such that they can be found easily and copied into the DVH QA excel spreadsheet in the tab MIM Second Check. The spreadsheet specifies which cell to paste the MIM DVH data for evaluation. The numerical evaluation of differences between Pinnacle's dose volume histogram calculation and MIM's dose volume histogram calculation was recorded in the tab Pin vs. MIM. The comparison between the two DVH calculation algorithms was accomplished



by directly comparing the structure volume calculated for the same dose bin with the results listed in Chapter 5.

## **4.2 MATLAB Second Check**

The purpose of developing two different secondary evaluation techniques for the Pinnacle dose volume histogram quality assurance results is to account for centers that do not have access to MIM. MATLAB is a more widespread program at the time of this research and as such should provide a good alternative evaluation tool for locations without MIM. The following procedure outlines the steps required to install and perform a secondary check with MATLAB.

The first step for the MATLAB procedure was to import the DICOM data for the relevant plan. In order to import DICOM files for evaluation in MATLAB the program CERR, pronounced ‘sir,’ was used. CERR stands for Computational Environment for Radiotherapy Research and is a software platform developed by Dr. Joseph O. Deasy and a team of programmers. CERR is a free software that has been funded by multiple grants by the US National Institutes of Health and is distributed under a GNU public license<sup>20</sup>. CERR is intended for research use only and cannot be used as a tool for clinical decisions. CERR is written entirely in MATLAB language and the executable files are user-editable. The CERR files were downloaded from the CERR website and installed.

Prior to describing the procedure for generating a dose volume histogram using MATLAB and CERR it is important to outline the DVH calculation method. The CERR wiki website describes the DVH calculation method<sup>19,20</sup>. CERR calculates a DVH using a modified grid based technique. Each CT voxel is defined by the dose grid. The voxel widths in the z direction are calculated to leave no gaps between CT slices. The space between adjacent CT slices is divided into two equal segments and included in the voxel of the previous slice and the voxel of the following slice. The dose to the voxel is determined by linear interpolations to the voxel center<sup>20</sup>. This calculation technique is a traditional method and represents a simplistic calculation that works well for a second check calculation.

While examining the dose volume histogram calculation method used in CERR, it was noted that the default grid size resolution was set to 2mm, which is different from the standard Pinnacle dose grid. In order to change the default setting the file `getDT.m` was modified from 0.2cm grid size to 0.4cm. The DVH export options also needed to be modified and this was accomplished by changing some of the default settings in the `CERROptions` file. The bin width was changed to match Pinnacle settings of 1cGy per bin. Every modification to CERR code was documented in the code with comments that were dated and signed. After these changes were saved the DICOM files were reimported so that the new dose grid resolution would be applied and the QA procedure was repeated. The effect of changing the dose grid resolution in CERR is explained in Chapter 5.

The following procedure outlines the steps involved in evaluating an exported treatment plan using CERR and MATLAB. For evaluating plans from Pinnacle the first step is to export the appropriate DICOM files to ARIA, open the ARIA DICOM import tab and determine the folder location of the exported DICOM files. Open this folder by copying the location from ARIA and pasting it into the search bar of the start menu. Select all of the DICOM files needed for evaluation and copy them to a flashdrive so that they can be transferred to the MATLAB computer. Transfer the DICOM files to a new folder with an appropriate name to the MATLAB computer. Once the DICOM files have been added to the MATLAB computer they can be accessed by MATLAB software. Type CERR in the MATLAB workspace and click ENTER. The CERR home screen will be displayed and select DICOM from the drop-down directory for import file type. Select the folder that contains the DICOM files for the relevant treatment plan and execute the import procedure. A screen will load that prompts the user to select the plan for import. After importing the DICOM files CERR will exit to the MATLAB workspace and must be reinitialized by typing in CERR. Select Viewer from the CERR home screen and load the MATLAB file that was just created by importing the DICOM files. This action will result in a similar display as Figure 4.1. From this step many different tools can be used to analyze and evaluate a plan imported to CERR. For the purpose of this quality assurance procedure the only functionality used is the dose volume histogram tool. In order to generate a DVH with CERR select Metrics and Dose Volume Histogram. A window that resembles Figure 4.2 will be generated. The user must input which structures to include on the dose volume histogram by selecting from the structure drop-down menu and clicking ADD DVH. For the purposes of this QA procedure, a

volumetric DVH was selected by checking the selection box and plotted as a cumulative DVH by clicking the Plot Cumulative button. This action generates a DVH as shown in Figure 4.3.

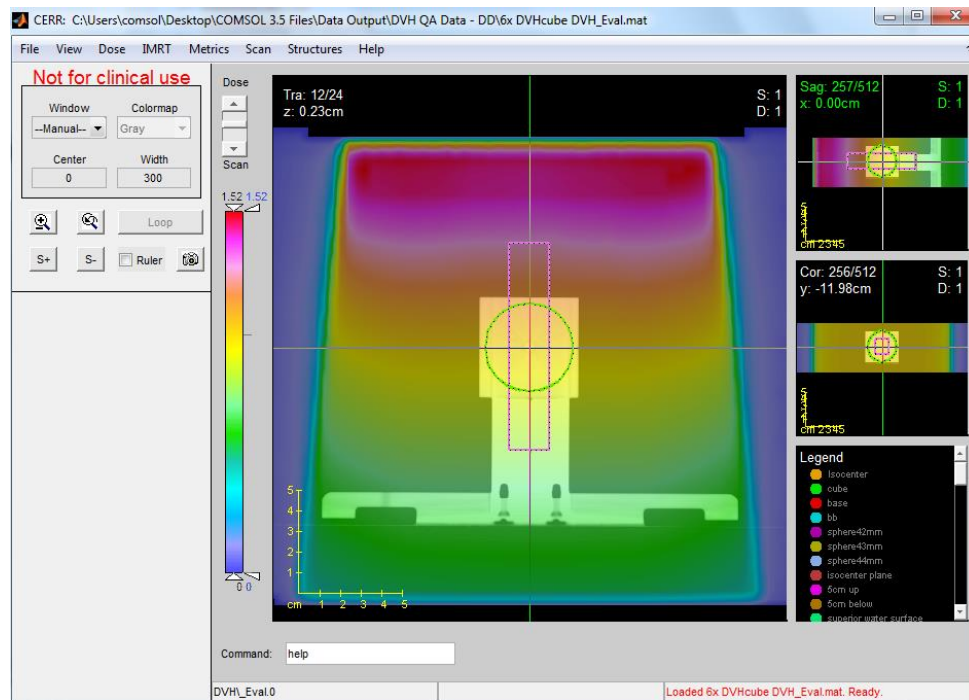


Figure 4.1: View of a Successfully Loaded Plan on CERR

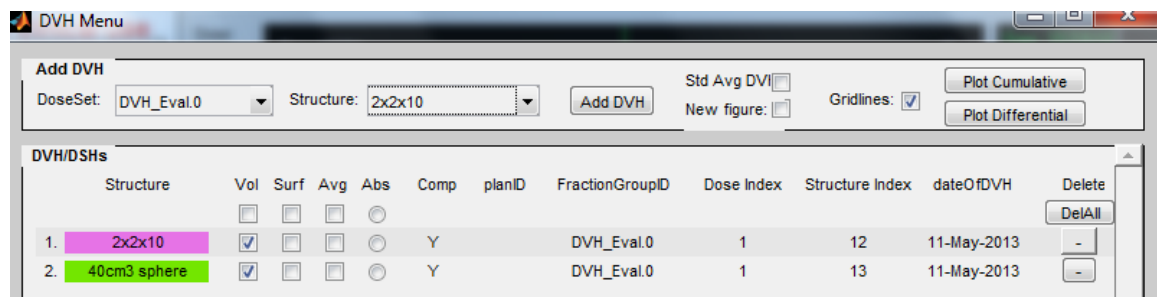


Figure 4.2: Dose Volume Histogram Structure Selection Screen in CERR

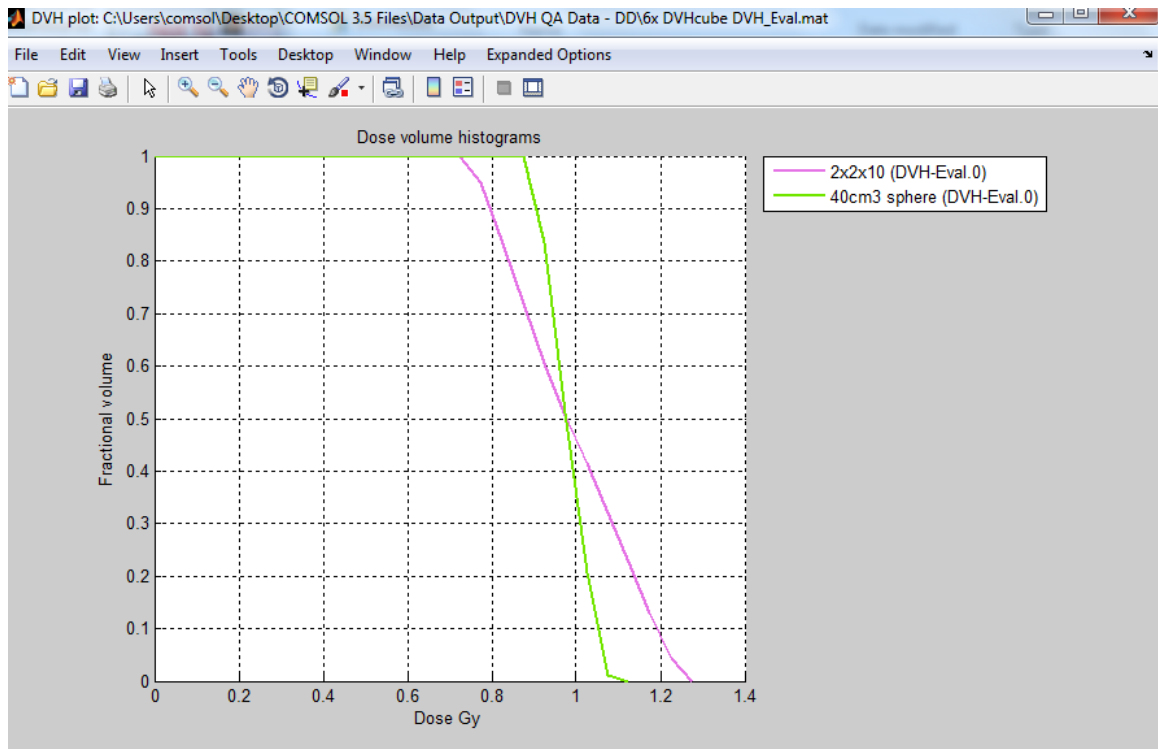


Figure 4.3: CERR Generated Dose Volume Histogram

For the purpose of obtaining data that could be evaluated in the QA spreadsheet it must be output as a data file. The user must select Expanded Options, select the volume for which to export data, and click export DVH. This step must be repeated for each volume of interest in the DVH and will save each data file as either a .xls or .csv file. This procedure was followed for each evaluated energy and the resulting data was saved to a flashdrive to be imported to the QA spreadsheet. The results of the MATLAB second check are listed in Chapter 5.

## Chapter 5

### Results

#### 5.1 Dose Volume Histogram Quality Assurance Primary Results

The results from completing the quality assurance procedures described in chapter 3 are listed in Table 5.1.

Table 5.1: Dose Volume Histogram Quality Assurance Results

	<b>2x2x10 Parallelepiped</b>		<b>Sphere</b>	
Energy	Max % Difference	Average % Difference	Max % Difference	Average % Difference
6 MV	1.44	0.73	2.14	0.53
10 MV	1.77	0.66	1.29	0.45
18 MV	1.36	0.60	1.93	0.54
6 FFF	1.41	0.48	2.14	1.20

Based on the calculations completed in the spreadsheet, the average percent difference between Pinnacle's dose volume histogram calculation and the expected dose to a known volume based on commissioned percent depth dose data is less than 1 percent for every energy except for the spherical ROI 6FFF field. This value should not be considered when discussing the overall average percent difference because the non-flat dose

distribution of the 6FFF field induces more uncertainty when evaluating a spherical volume of interest than a parallelepiped due to the structure of the ROI. With the removal of the 6FFF spherical percent difference the average percent difference found from Pinnacle's dose volume histogram calculation is no greater than 0.73 percent. This result demonstrates a good agreement between the Pinnacle dose volume histogram algorithm and the commissioned beam output data. The following figures demonstrate the fit between the dose volume histogram calculation and the expected dose to a known volume based on commissioned percent depth dose data. The standard x and y axis are reversed from the normal DVH depiction in order to simplify the visual representation of the dose calculated for precise volumes of the ROI structure. This was done to highlight the evaluation technique of comparing calculated and measured doses to a known volume.

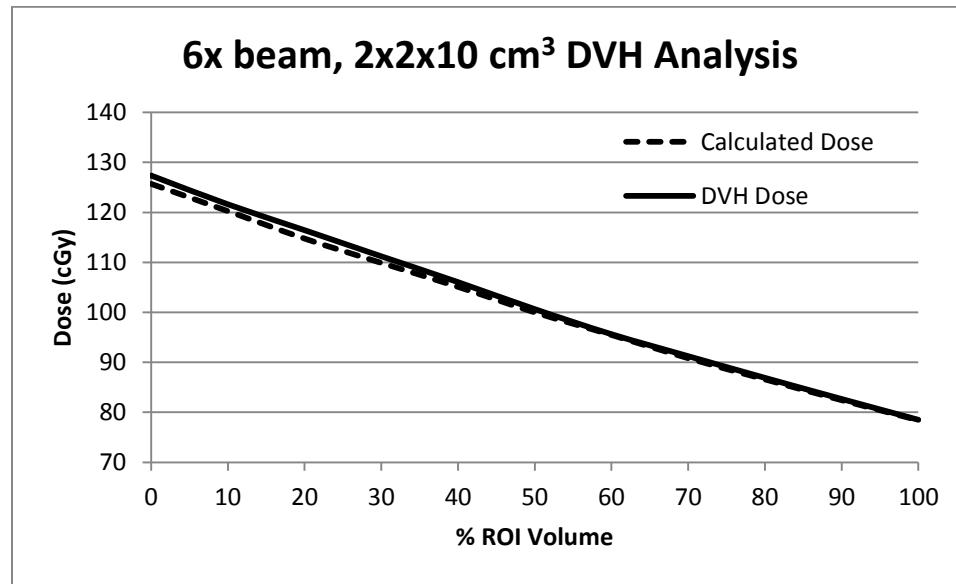


Figure 5.1: Comparison of 6x DVH Dose Results and Calculated Dose Results from Commissioned PDD Data for 2x2x10 cm<sup>3</sup> ROI Structure

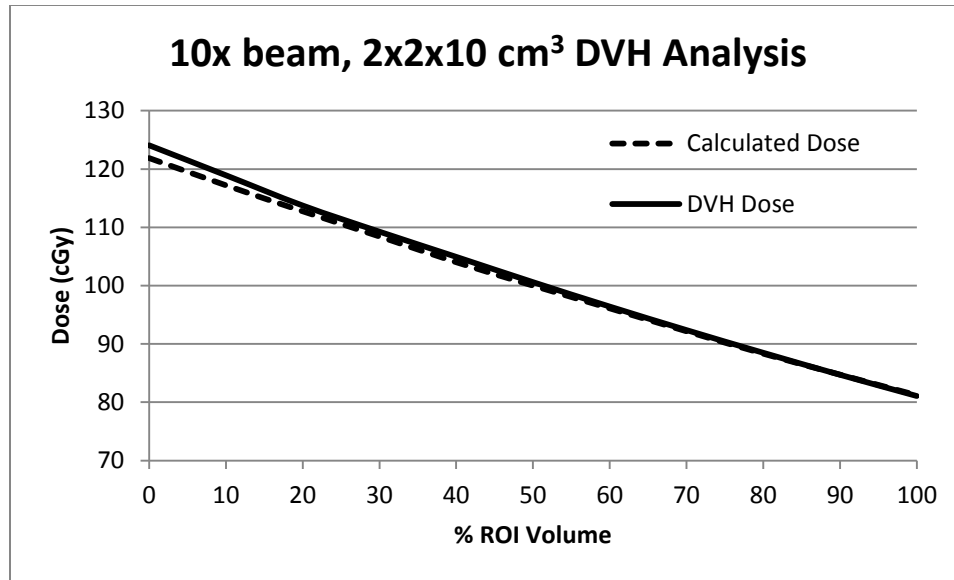


Figure 5.2: Comparison of 10x DVH Dose Results and Calculated Dose Results from Commissioned PDD Data for 2x2x10 cm<sup>3</sup> ROI Structure

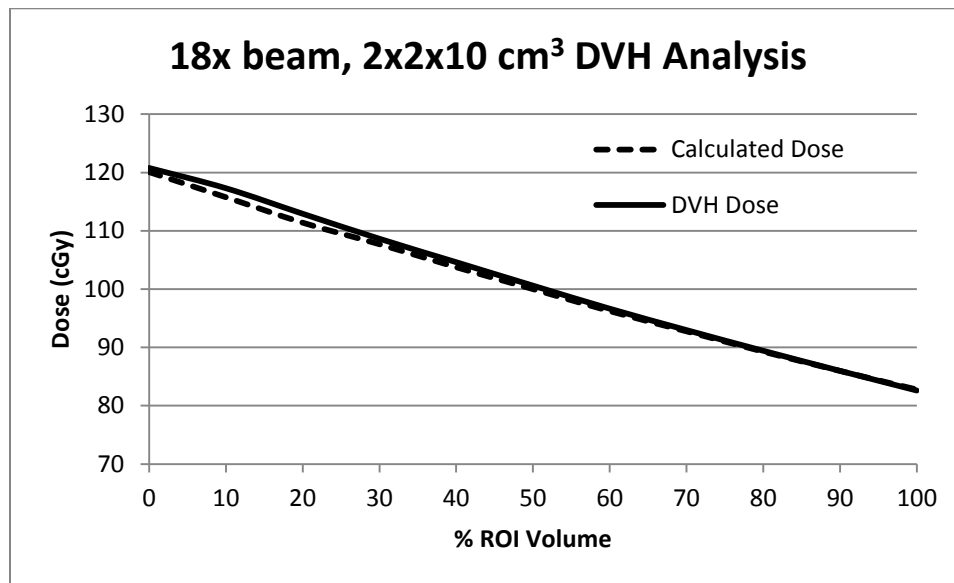


Figure 5.3: Comparison of 18x DVH Dose Results and Calculated Dose Results from Commissioned PDD Data for 2x2x10 cm<sup>3</sup> ROI Structure



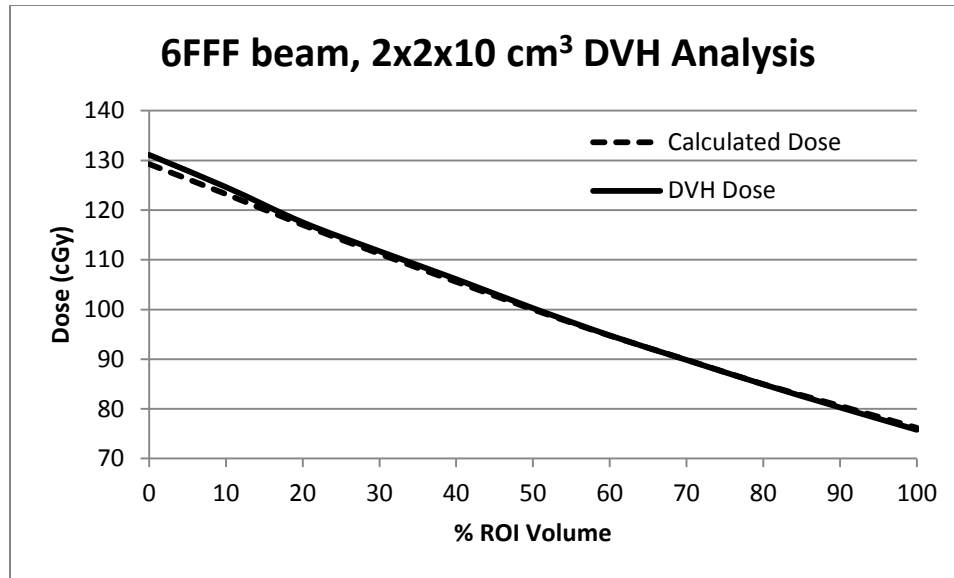


Figure 5.4: Comparison of 6FFF DVH Dose Results and Calculated Dose Results from Commissioned PDD Data for 2x2x10 cm<sup>3</sup> ROI Structure

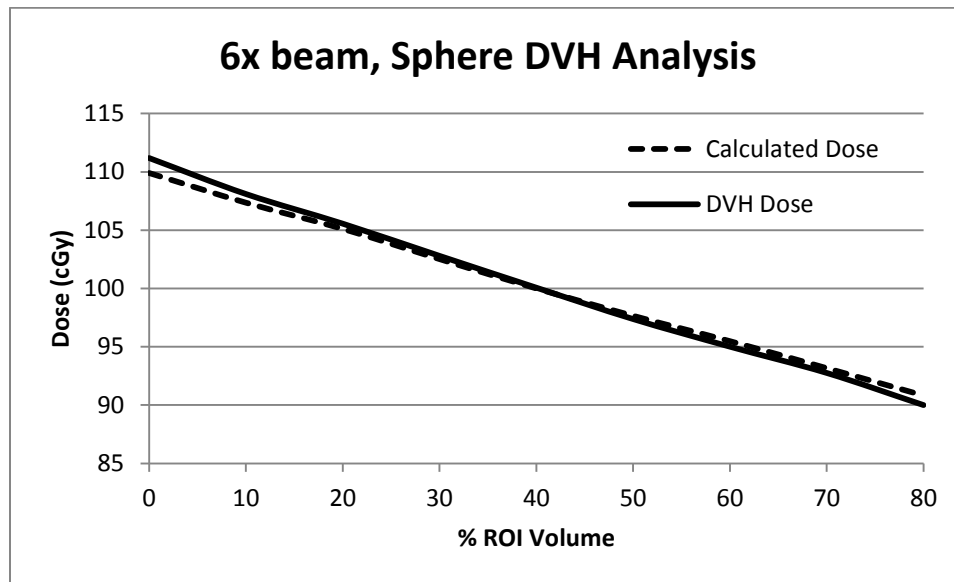


Figure 5.5: Comparison of 6x DVH Dose Results and Calculated Dose Results from Commissioned PDD Data for Sphere ROI Structure

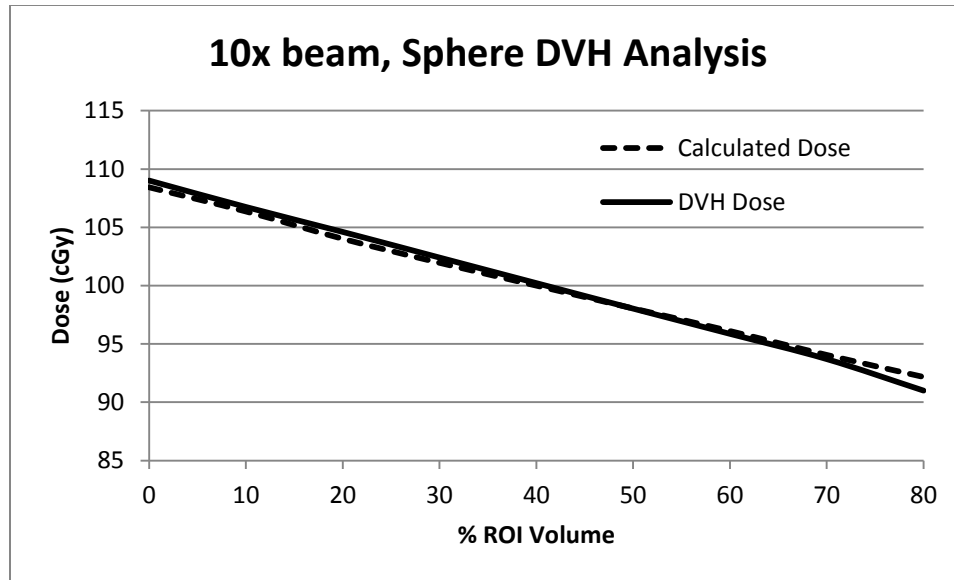


Figure 5.6: Comparison of 10x DVH Dose Results and Calculated Dose Results from Commissioned PDD Data for Sphere ROI Structure

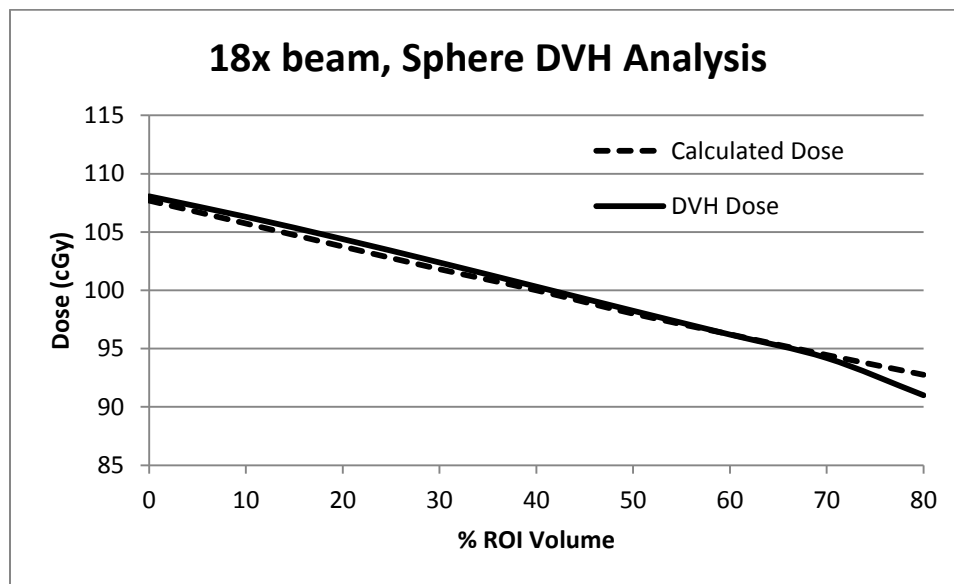


Figure 5.7: Comparison of 18x DVH Dose Results and Calculated Dose Results from Commissioned PDD Data for Sphere ROI Structure

An average percent difference of less than 1% is an acceptable result for the quality assurance procedure to be considered successful. This result should be checked with either the MIM or MATLAB second check procedure in order to confirm calculation accuracy.

## 5.2 Off-axis Evaluation Results

The effect of ROI positioning with respect to the dose grid was tested by shifting the ROI off axis by three set values. The results for this test show that the greatest difference was caused when the ROI was shifted 1.5cm off axis, corresponding to a 3mm shift with respect to the 4mm linear dimension of the dose grid. The largest difference was found for the 6FFF beam however this was to be expected due to the non-flat dose distribution produced by 6FFF beams. For this test the 6FFF data is unimportant and thus will not be considered. Table 5.2 contains the numerical results for the off axis evaluation tests.

Table 5.2: Average Percent Differences due to Shifting ROI Structures Off-Axis

Energy	Average % Difference		
	0.5cm offset	1.0cm offset	1.5cm offset
6x	0.19	0.61	0.78
10x	0.16	0.86	2.80
18x	0.05	0.59	4.79
6FFF	0.54	2.43	5.57

The greatest source of difference for the off axis evaluation was the final dose bin for the highest dose being delivered to the smallest volume of the ROI at the base of the DVH tail. This difference is due to a combination of effects. Beam flatness and symmetry is more influential with the greatest shift of 1.5cm which is reflected in the results. Another reason for greater percent difference values is that at the tail of the DVH very small volumes are being compared so the resulting percent difference can be large but the effect on the DVH can be minimal. Table 5.3 contains the results of this test when removing this value from the percent difference calculation. By removing the final dose bin from the calculation the numerical results of the off axis evaluation match more closely the dose volume histogram results in Figures 5.8 through 5.11.

Table 5.3: Average Percent Differences due to Shifting ROI Structures Off-Axis without the Error from Final Dose Bin in DVH Tail Region

Energy	Average % Difference Without Tail		
	0.5cm offset	1.0cm offset	1.5cm offset
6x	0.19	0.61	0.78
10x	0.18	0.82	1.86
18x	0.06	0.41	1.05
6FFF	0.44	1.99	4.50

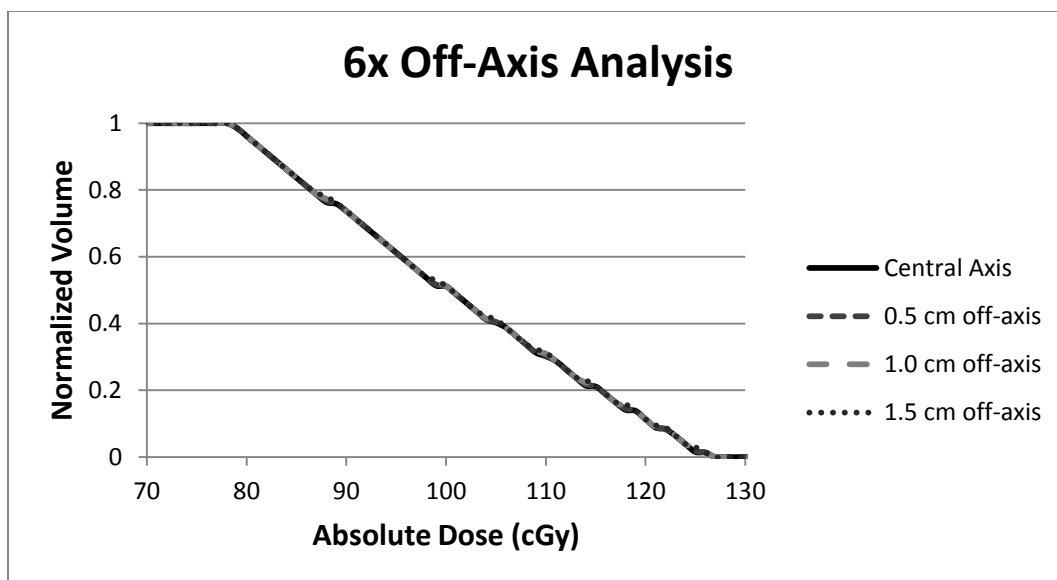


Figure 5.8: Dose Volume Histogram for a 6x Beam Exposing the 2x2x10 Parallelepiped at Various Positions Relative to the Central Beam Axis

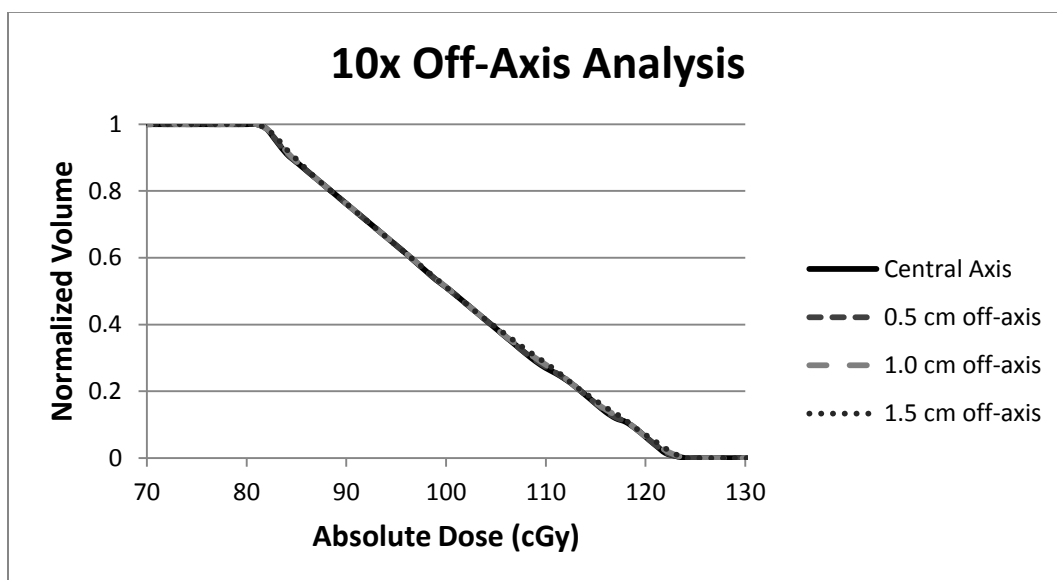


Figure 5.9: Dose Volume Histogram for a 10x Beam Exposing the 2x2x10 Parallelepiped at Various Positions Relative to the Central Beam Axis

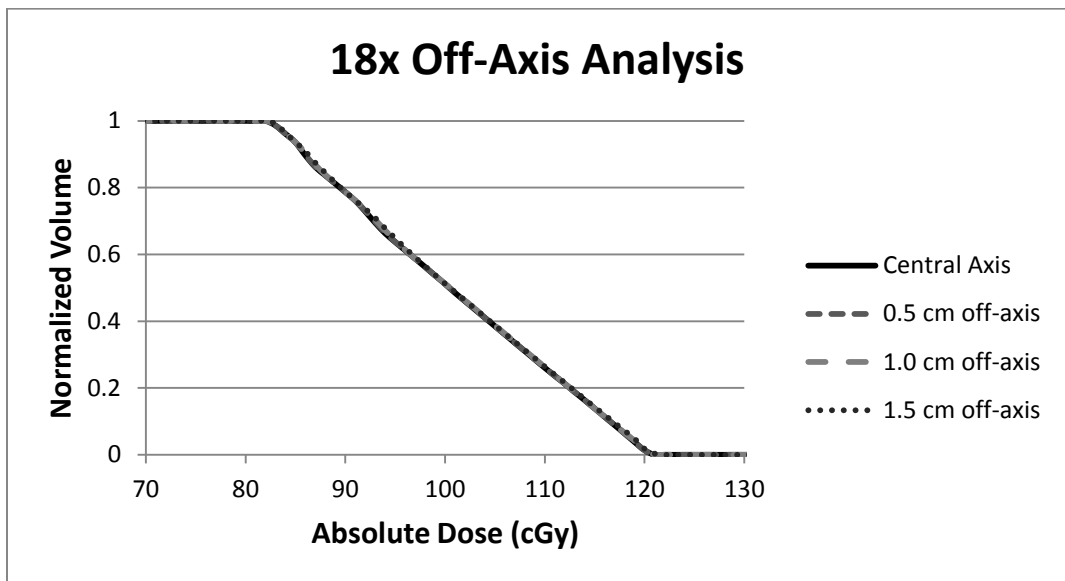


Figure 5.10: Dose Volume Histogram for a 18x Beam Exposing the 2x2x10 Parallelepiped at Various Positions Relative to the Central Beam Axis

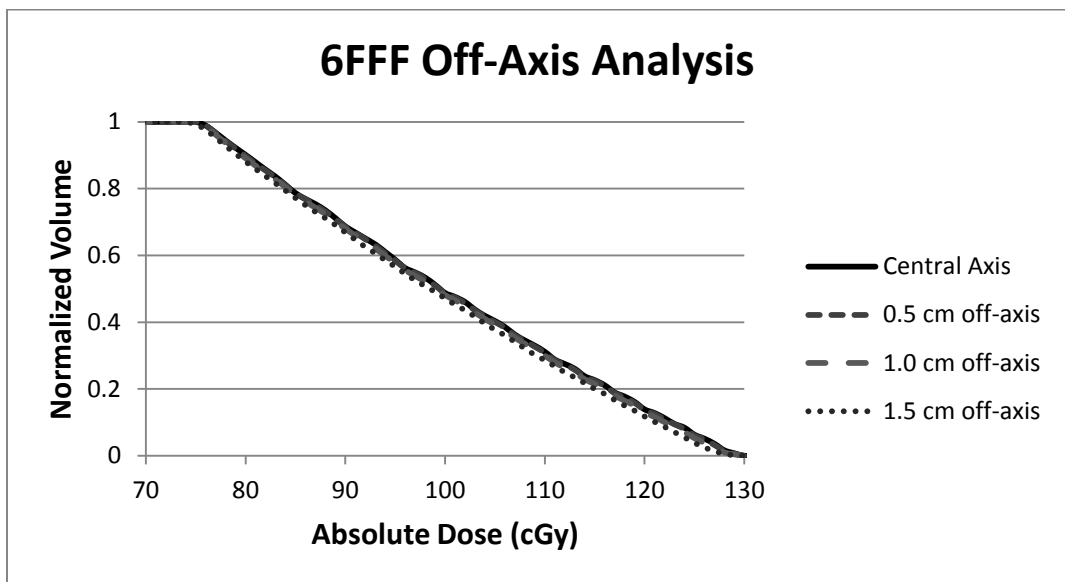


Figure 5.11: Dose Volume Histogram for a 6FFF Beam Exposing the 2x2x10 Parallelepiped at Various Positions Relative to the Central Beam Axis

### 5.3 Dose Grid Size Evaluation Results

For the large parallelepiped,  $2 \times 2 \times 10 \text{ cm}^3$ , the greatest percent difference induced by varying the dose grid was 1.1% with an average effect of 0.32%. Similar results were found for the smaller ROI with the max percent difference induced by varying the dose grid of 1.1% with an average effect of 0.34%. The full numerical results for the first dose grid resolution evaluation are listed in Table 5.4.

Table 5.4: Primary Dose Grid Evaluation Results

	Percent Difference for $2 \times 2 \times 10$			Percent Difference for Small ROI		
	2mm DG	3mm DG	5mm DG	2mm DG	3mm DG	5mm DG
Average	0.21	0.32	0.27	0.25	0.34	0.26
Maximum	0.69	1.09	0.83	1.10	1.10	1.00

The average percent difference induced by varying the dose grid for a uniform dose distribution was less than 0.3% for both ROIs. Figures 5.12 and 5.13 demonstrate the quality of dose volume histogram calculation accuracy between the various dose grid resolution settings.

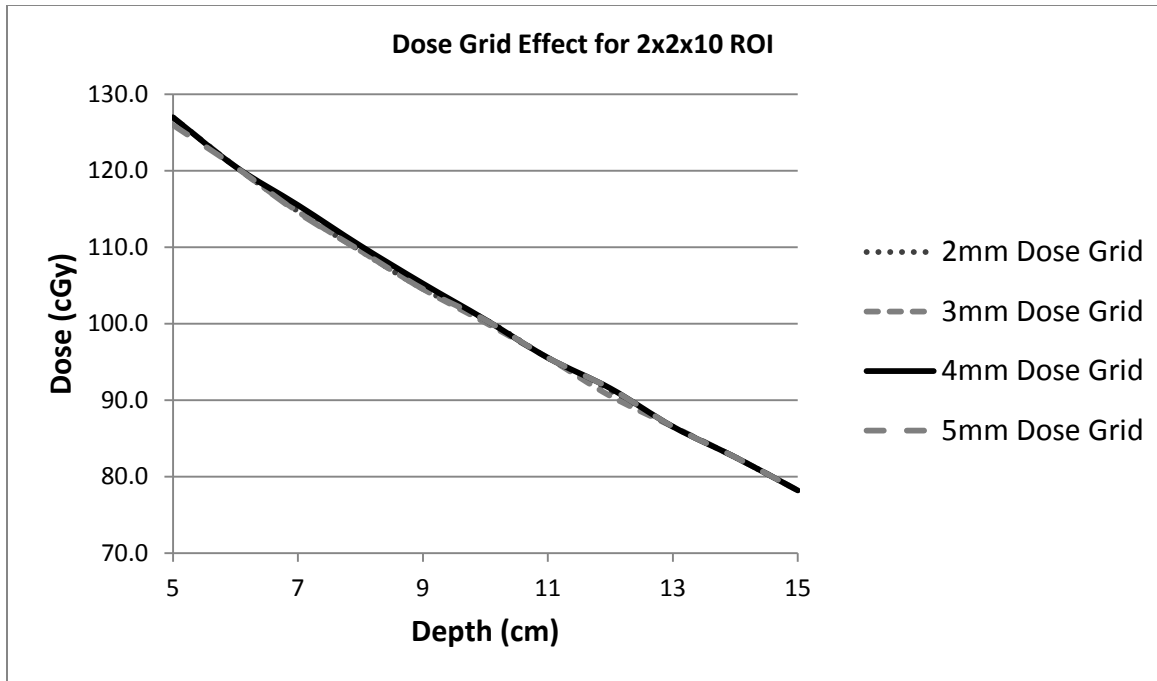


Figure 5.12: Dose Volume Histograms Calculated with Different Dose Grid Resolutions for the Large ROI of 40cm<sup>3</sup>

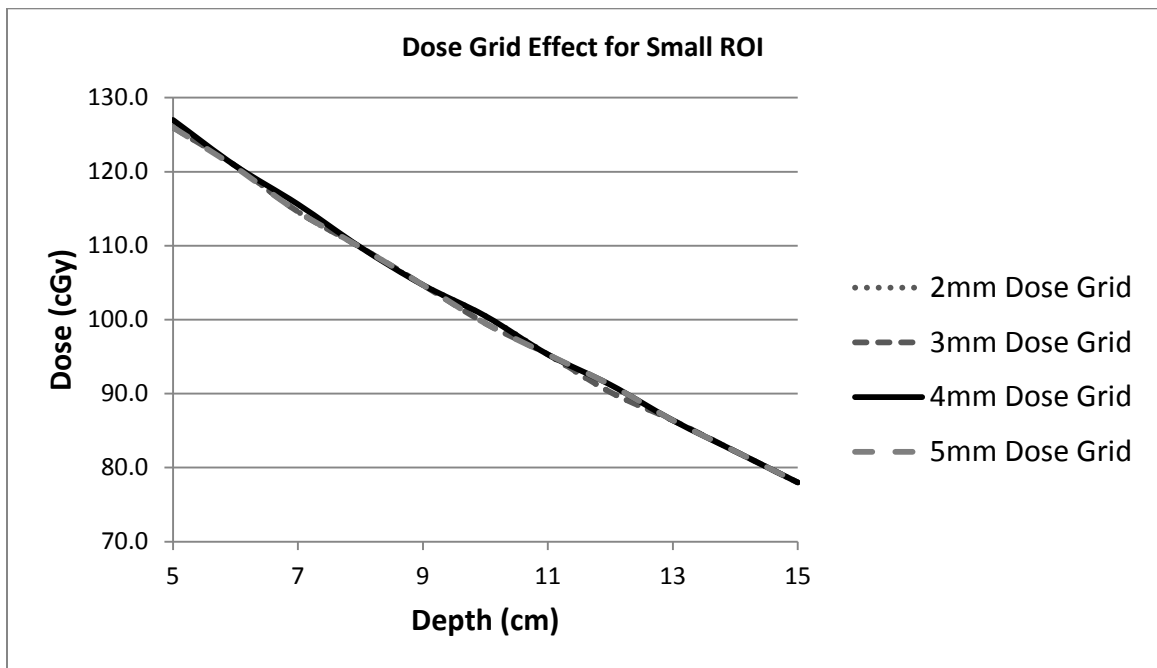


Figure 5.13: Dose Volume Histograms Calculated with Different Dose Grid Resolutions for the Small ROI of 0.64cm<sup>3</sup>



The hypothesis that instigated the design of a secondary test with a region of high dose gradient was that the importance of dose grid resolution would increase under such conditions. The outcomes of the test confirm this hypothesis. The test resulted in two different sets of data for the average percent difference between the various dose grid sizes. The solution does not include the percent difference between the very tail of the DVH and the reference value. The DVH calculation displays drastically different values for normalized volume for the highest dose bins. This region is not of much importance however when a DVH is evaluated and as such the primary conclusions have these values excluded. Table 5.4 contains the numerical results of this test.

Table 5.5: Dose Grid Evaluation Results with High Dose Gradient

	Average % Difference for Large ROI			Average % Difference for Small ROI		
	2mm DG	3mm DG	5mm DG	2mm DG	3mm DG	5mm DG
No Tail	2.16	1.84	2.43	1.70	2.12	2.06
With Tail	5.70	11.10	5.90	7.68	4.36	5.54

The average percent difference that is induced when changing the dose grid resolution for a region of high dose gradient is roughly 2 percent. The similarity between the calculated DVHs is also apparent in figures 5.14 and 5.15.

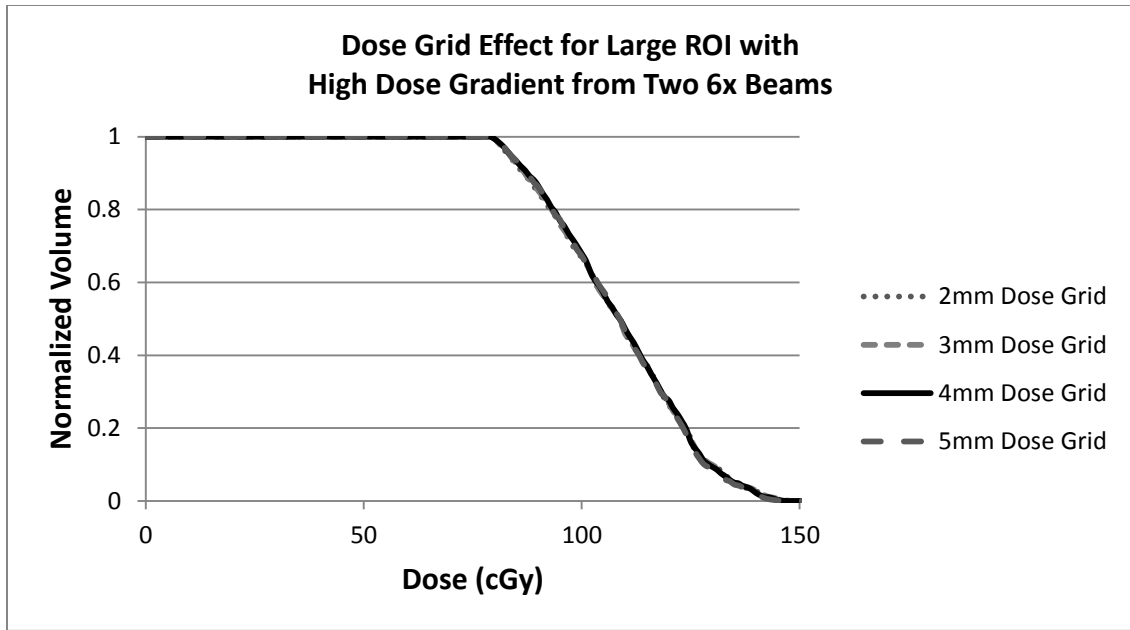


Figure 5.14: Dose Volume Histograms Calculated with Different Dose Grid Resolutions for a Region of High Dose Gradient to the Large ROI of 40cm<sup>3</sup>

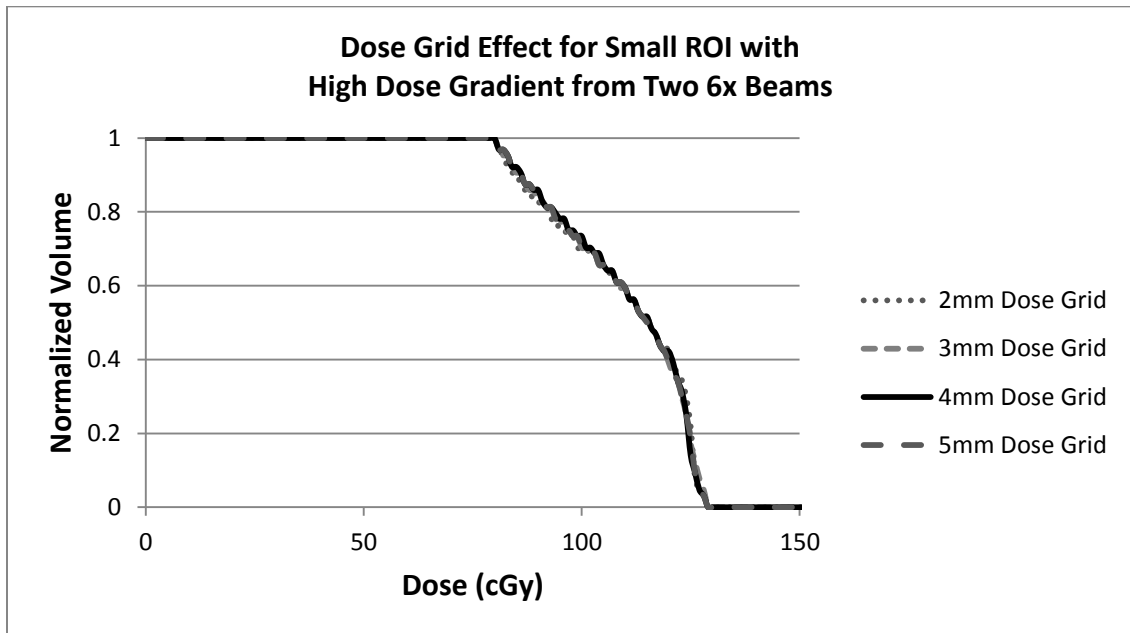


Figure 5.15: Dose Volume Histograms Calculated with Different Dose Grid Resolutions for a Region of High Dose Gradient to the Small ROI of 0.64cm<sup>3</sup>

## 5.4 CT Slice Thickness Evaluation Results

The standard CT slice thickness used for most scans at the University of Toledo is 3mm. The DVH tabular data results for the three scans were copied into the excel QA spreadsheet and evaluated with the 3mm DVH data used as the reference value. Table 5.6 is the average percent difference for each energy and each CT slice thickness. The average percent difference between the 0.75mm slice thickness and 3.0mm slice thickness across the three energies was shown to be less than 1.5%. The average percent difference between the 1.5mm slice thickness and 3.0mm slice thickness across the three energies was shown to be less than 2.25%. The average percent difference between the different CT slice thickness settings was less than 2%.

Table 5.6: CT Slice Thickness Evaluation Results

Average Percent Difference		
Energy	0.75 mm	1.5 mm
6x	1.02	1.92
10x	1.91	2.73
18x	1.44	2.03

Figures 5.16 through 5.18 are the dose volume histograms of each CT slice thickness for 6x, 10x, and 18x beam energies.

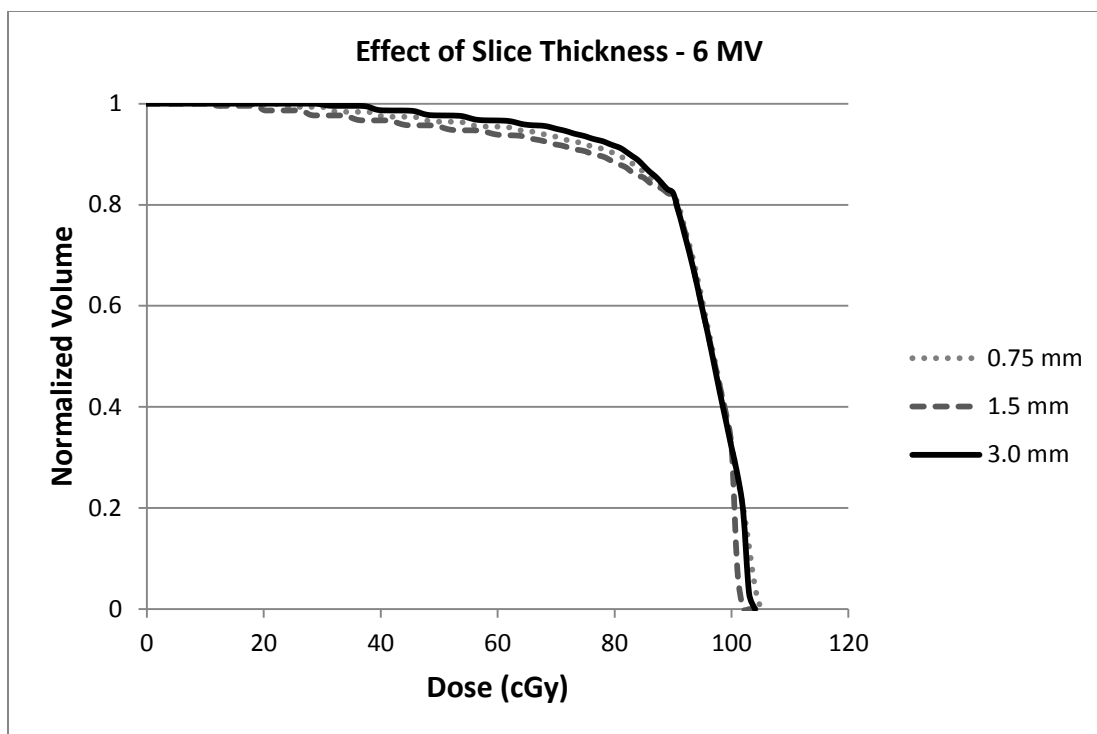


Figure 5.16: Dose Volume Histogram for Three CT Slice Thickness Settings for 6 MV

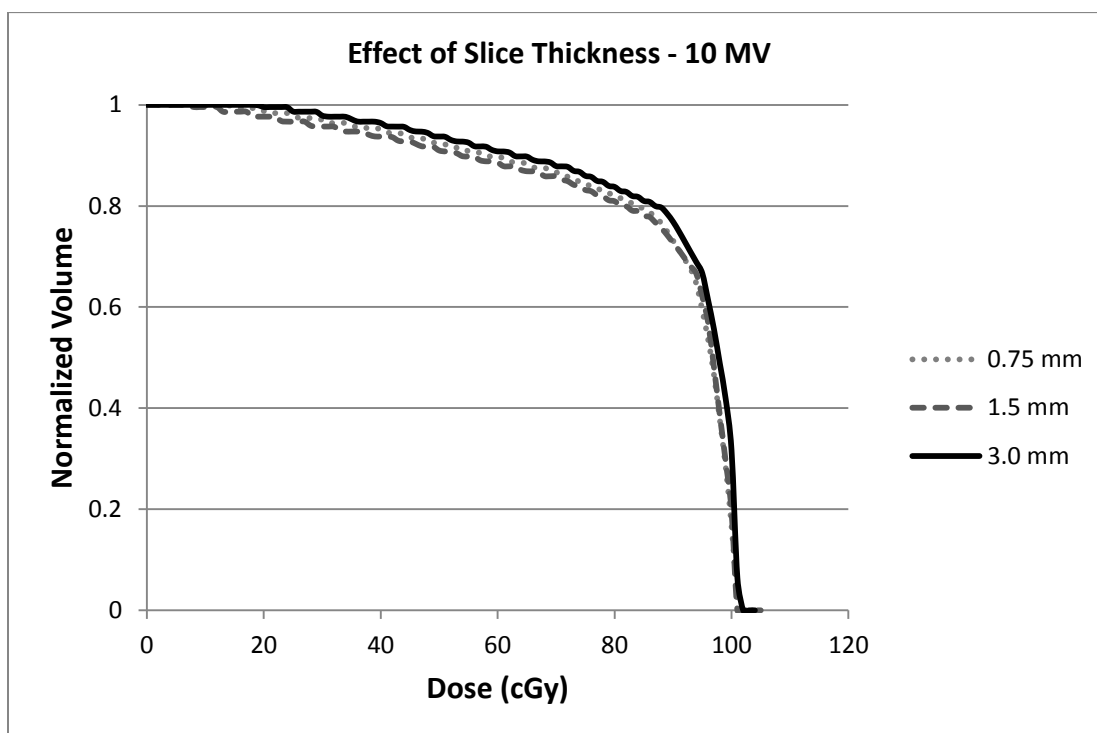


Figure 5.17: Dose Volume Histogram for Three CT Slice Thickness Settings for 10 MV

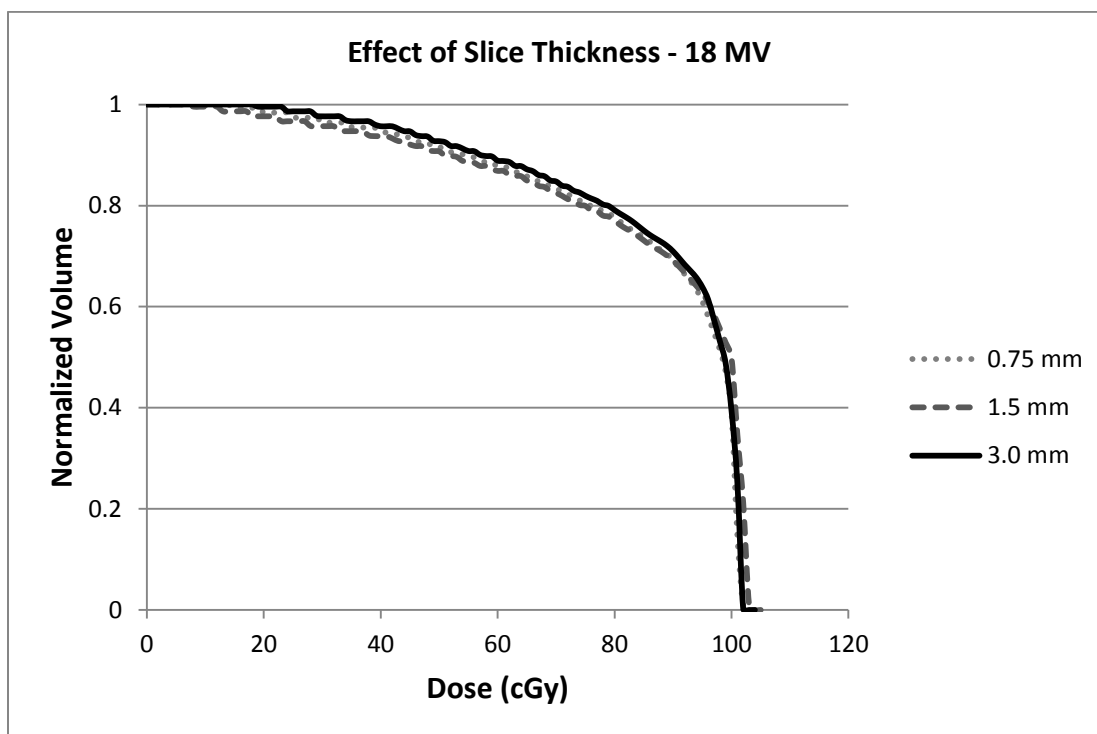


Figure 5.18: Dose Volume Histogram for Three CT Slice Thickness Settings for 18 MV

## 5.5 MIM Second Check Results

The MIM second check procedure resulted in two sets of data that provided insights into the difference in dose volume histogram calculation methods between Pinnacle and MIM. The first set of results was found by evaluating the absolute volume receiving a known amount of dose. This comparison resulted in an average 2.88% difference for the parallelepiped and 1.89% difference for the spherical volume as shown in Table 5.7.

Table 5.7: MIM Second Check Results for Absolute Volume Comparison

For Absolute Volume	Max % Difference	Average % Difference
Parallelepiped	14.52	2.88
Sphere	5.03	1.89

The maximum percent difference was found in calculation of the volume receiving the maximum dose (DVH tail). The overall agreement between MIM and Pinnacle does not suggest a systematic difference between the two dose volume histogram calculation methods.

The second set of results was found when comparing the normalized volume receiving a known amount of dose. This comparison is more relevant to the accuracy of the overall DVH calculation because a standard cumulative DVH is shown with normalized volume. The results of this comparison are listed in Table 5.8.

Table 5.8: MIM Second Check Results for Normalized Volume Comparison

For Normalized Volume	Max % Difference	Average % Difference
Parallelepiped	11.74	0.87
Sphere	0.26	0.96

The lower percent differences for the comparison of normalized volume than the comparison of absolute volume is evidence that the primary source of error for the absolute volume comparison is from ROI volume calculation. This again implies that MIM utilizes a different volume calculation technique than Pinnacle.

## 5.6 MATLAB Second Check Results

Two full evaluations were completed following the procedure outlined in Chapter 4 for the MATLAB second check test. The first evaluation was taken with the dose grid resolution set to the default 2mm in CERR. Table 5.9 and Figure 5.19 contain the second check results and demonstrate the agreement between MATLAB and Pinnacle for DVH calculation when MATLAB is using a 2mm (default) resolution and Pinnacle is using 4mm.

Table 5.9: MATLAB Second Check Results for 2mm Dose Grid Resolution

Energy	Structure	% Difference
6x	2x2x10	2.38
	Sphere	2.36
10x	2x2x10	2.37
	Sphere	2.43
18x	2x2x10	2.38
	Sphere	2.44
6FFF	2x2x10	2.33
	Sphere	2.40
Average % Difference for 2x2x10		2.37
Average % Difference for Sphere		2.41

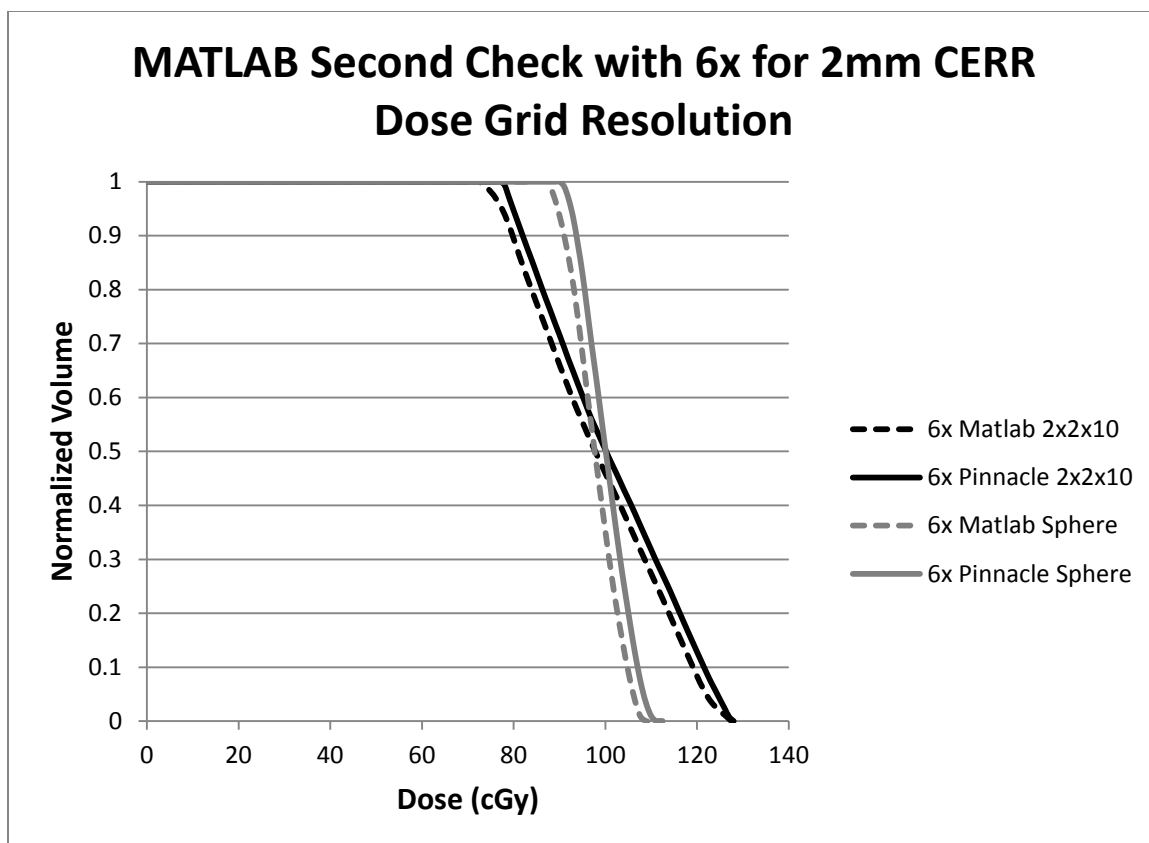


Figure 5.19: Comparison of 6x DVH Dose Results from Pinnacle and MATLAB with a 4mm Dose Grid in Pinnacle and a 2mm Dose Grid in MATLAB

Table 5.9 shows that the average percent difference for this test was roughly 2.4%. This value was larger than expected and was concerning enough to motivate further study. At this stage the dose grid resolution difference was noted and the code was modified to calculate DVHs with a 4mm dose grid in CERR as well as in Pinnacle. After making the necessary adjustments explained in Chapter 4, the second check procedure was repeated using the new settings and the results are provided in Table 5.10 and Figure 5.20.



Table 5.10: MATLAB Second Check Results for 4mm Dose Grid Resolution

Energy	Structure	% Difference
6x	2x2x10	0.39
	Sphere	0.40
10x	2x2x10	0.39
	Sphere	0.42
18x	2x2x10	0.41
	Sphere	0.43
6FFF	2x2x10	0.35
	Sphere	0.39
Average % Difference for 2x2x10		0.38
Average % Difference for Sphere		0.41

An interesting result from this test was that the dose grid resolution setting dramatically affected the results for the dose volume histogram in CERR. This result was somewhat surprising because the effect of varying the dose grid resolution was evaluated in Pinnacle and was shown to be far less prominent. The increased effect of changing the dose grid resolution in CERR demonstrates that it uses a different DVH calculation algorithm than Pinnacle. After changing the dose grid resolution of CERR to match that of Pinnacle the average percent difference was shown to be roughly 0.4%. This demonstrates excellent agreement between CERR and Pinnacle. CERR has been shown to agree well with most treatment planning systems however some difficulties have been shown between CERR and NOMOS Peacock<sup>21</sup>. This agreement serves as a justification of the results of the quality assurance procedure.

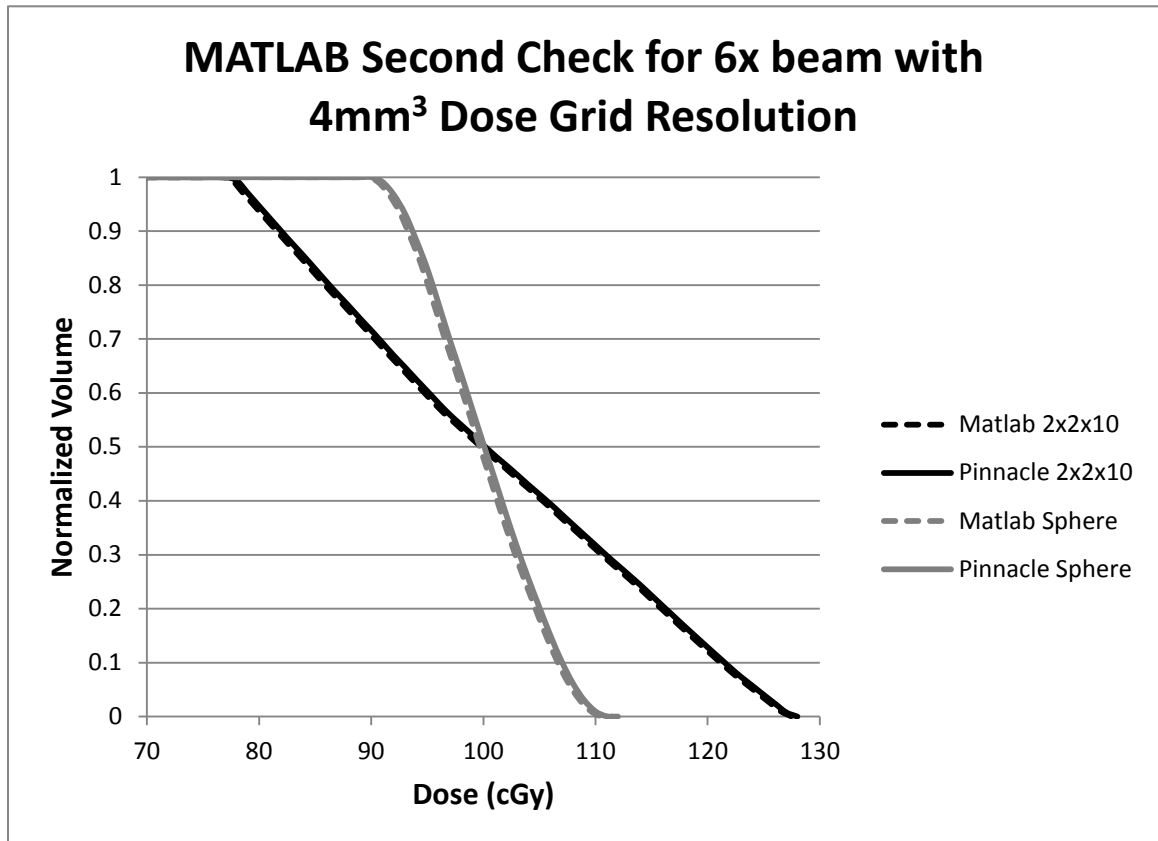


Figure 5.20: Comparison of 6x DVH Dose Results from Pinnacle and MATLAB with a 4mm Dose Grid in Pinnacle and a 4mm Dose Grid in MATLAB

## **Chapter 6**

### **Conclusions**

The quality assurance evaluation results demonstrate for all energies an average difference less than 1% between the dose volume histogram calculated in Pinnacle and the commissioned machine data for percent depth dose measurements. Currently there is no published tolerance for dose volume histogram accuracy; however the result of less than 1% difference demonstrates that the Pinnacle dose volume histogram calculation is accurate. The developed quality assurance procedure insures that the calculated dose volume histogram can be confidently utilized as a plan evaluation metric.

The results for the off axis evaluation show that for the 0.5cm and 1.0cm shifts off axis there is an average difference less than 1%. The 1.5cm shift off axis induced an average difference less than 2% when disregarding the final data point at the base of the tail of the DVH. These results show that with the dose grid resolution set to the standard value of 4mm small shifts on the order of 1 or 2mm, do not induce a significant error in the dose volume histogram. A shift between 3 and 4mm will cause a 1% to 2% difference in the DVH calculation. This difference will primarily be relevant when re-planning patient treatments with image guided adaptive radiation therapy or a new CT and comparing the resulting DVH to the previous DVH. Based on this research, factoring in

up to a 2% difference between a re-calculated and the original DVH would be recommended.

The evaluation of the effect of changing the dose grid resolution for a homogenous dose distribution was found to produce less than 0.4% difference between DVHs. This result confirms the hypothesis that for a homogenous field the effect of the dose grid selection is minimal. The high dose gradient test was done in order to evaluate the impact of the dose grid resolution when voxels were exposed to varying radiation conditions. The results of the high dose gradient dose grid test show that an average difference of approximately 2% was induced in the calculated DVH, suggesting that care should be taken when comparing dose volume histograms for regions of high dose gradient that were calculated using different dose grid resolutions.

The effect of varying the CT slice thickness on resulting dose volume histogram calculations was found to cause on average a 2% difference. This uncertainty is not present in a standard treatment plan because they are normally completed using a fixed CT slice thickness setting. This 2% difference should be taken into consideration when comparing treatment plans from external sites with different scan settings or different CT modalities. If this is taken into account the DVH is usable as an accurate plan evaluation tool for CTs of different slice thickness settings.

The purpose of second check verifications is to insure the accuracy of Pinnacle's dose volume histogram calculation compared to other calculation techniques. The DVH comparison of Pinnacle and MIM Maestro for normalized volumes resulted in an average difference of less than 1%. This result demonstrates a close agreement between the

calculation algorithms of Pinnacle and MIM. The MATLAB second check procedure was designed to be an alternative check for facilities that do not have access to MIM Maestro. The results from the MATLAB second check procedure demonstrate an average difference less than 0.5% between Pinnacle DVH values and the DVH calculated by CERR in MATLAB. Both second check procedures using MIM and MATLAB demonstrate close agreement with the Pinnacle dose volume histogram calculation results. This confirms that the Pinnacle DVH calculation algorithm is sound.

This quality assurance procedure has been designed for use after the commissioning of a new linear accelerator or after any update to the beam model in a treatment planning system. The physicist must only perform the primary procedure outlined in Chapter 3 Section 1 for DVH Analysis and one of the two secondary check procedures in order to complete a routine implementation of the dose volume histogram quality assurance procedure. By following the procedures outlined in this thesis, the physicist should have no trouble implementing the whole test in as little time as two hours. The only extra step that will be required of the physicist is copying the relevant QA plan into the new machine institution in Pinnacle and changing the beam model in the plan. After this step the export, spreadsheet analysis, and second check procedure should be straightforward. This QA procedure was designed to greatly simplify the analysis of DVH accuracy while accomplishing all required tests in a short period of time.

## References

<sup>1</sup>Slater J M, “*From X-Rays to Ion Beams: A Short History of Radiation Therapy*,” Chapter 1 of U. Linz (ed.), *Ion Beam Therapy, Biological and Medical Physics*, Biomedical Engineering, DOI 10.1007/978-3-642-21414-1 1, Springer-Verlag, 2012

<sup>2</sup>Wilhelm Conrad Röntgen – Biography, Nobelprize.org, 21 May, 2013, [http://www.nobelprize.org/nobel\\_prizes/physics/laureates/1901/rontgen-bio.html](http://www.nobelprize.org/nobel_prizes/physics/laureates/1901/rontgen-bio.html)

<sup>3</sup>Browne, John C, “*A Brief History of High Power RF Proton Linear Accelerators*,” Los Alamos National Laboratory, <http://www.osti.gov/bridge/servlets/purl/475578-d5w2xR/webviewable/475578.pdf>

<sup>4</sup>Shipley W U, Tepper J E, Prout G R, Verhey L J, Mendiondo O A, Goitein M, Koehler A M and Suit H D, “*Proton radiation as boost therapy for localized prostatic carcinoma*,” 1979, JAMA 241, 1912–5

<sup>5</sup>Chen G, 1988, Ink J. Radiation Oncology Biol. Phys, Vol. 14. pp. 1319-1320

<sup>6</sup>Mayles, Philip, Alan Nahum, and Jean-Claude Rosenwald, “*Handbook of Radiotherapy Physics*,” 1st Ed. New York: Taylor & Francis, 2007. Print.

<sup>7</sup>Perez, Carlos, and Luther Brady, “*Principles and Practice of Radiation Oncology*,” 5th Ed. Philadelphia: Lippincott Williams & Wilkins, 2008. Print.

<sup>8</sup>Gunderson, Leonard, and Joel Tepper, “*Clinical Radiation Oncology*,” 2nd Ed. Philadelphia: Churchhill Livingstone, 2007. Print.

<sup>9</sup>Niemierko A, Goitein M, “*Random sampling for evaluating treatment plans*,” Med Phys 1990;17:753–762.

<sup>10</sup>Henríquez, F C, Castrillón S V, “*A Novel Method for the Evaluation of Uncertainty in Dose-Volume Histogram Computation*,” Int. J. Radiation Oncology Biol. Phys., Vol.70, No.4, pp.1263-1271, 2008

<sup>11</sup>ACR, “*ACR Technical Standard for The Performance of Radiation Oncology Physics for External Beam Therapy*”, Revised 2010, Resolution 7

<sup>12</sup>ACR, “*ACR –ASTRO Practice Guideline for 3D External Beam Radiation Planning and Conformal Therapy*”, Revised 2011, CSC/BOC

<sup>13</sup>Task Group No. 53, “*Quality assurance for clinical radiotherapy treatment planning*” American Association of Physicist in Medicine, Madison: Medical Physics Publishing, 1998

<sup>14</sup>Gossman M S, Bank M I, “*Dose-volume histogram quality assurance for linac-based treatment planning systems*,” J Med Phy

<sup>15</sup>Goudry B, DVHtoTXT Script Files.

<http://www.medphysfiles.com/index.php?name=Downloads&file=details&id=84>

<sup>16</sup>"MIM Software." . MIM Software Inc., n.d. Web. 1 Jun 2013.

<<http://www.mimsoftware.com>>.

<sup>17</sup>"MATLAB - The Language of Technical Computing." . The MathWorks, Inc., n.d.

Web. 1 Jun 2013. <<http://www.mathworks.com/products/matlab>>.

<sup>18</sup>Veld A A V, Bruinvis I A D, "*Influence of shape on the accuracy of grid-based volume calculations,*" Med. Phys. 22 (9), 1995

<sup>19</sup>"CERRWiKi." . Amy Wang Studio, 10 Dec 2012. Web. 1 Jun 2013.

<<http://cerr.info/cerrwiki/index.php/CERR?w=CERRWiKi>>.

<sup>20</sup>CERR, Deasy J, "*A Computational Environment for Radiotherapy Research,*"

<http://www.cerr.info/about.php>

<sup>21</sup> Deasy, Joseph. "CERR: A computational environment for radiotherapy research."

Medical Physics. 30.5 (2003): 979-985. Print.



## **Appendix A – Procedure for DVH Text to Script**

In order to analyze dose volume histograms developed on Pinnacle, one must be able to export the tabular DVH data to a readable format such as a text file. This was accomplished by modifying a preexisting script found on MedPhysFiles created by Bert Goudry<sup>7</sup>. The following procedure runs the DVH to Text script and must be used to export Pinnacle DVH data to be put into the quality assurance spreadsheet.

The following script file locations were set for the University of Toledo and will have to be customized by the user upon downloading the export script from MedPhysFiles. The script files can be found under the directory `usr/local/adacnew/PinnacleSitedata/Scripts/DavenportDVH`. To analyze a selected dose volume histogram and create a text file select utilities, scripting, usr, local, adacnew, PinnacleSitedata, scripts, DavenportDVH and select DVHOutputtoTxtStart. A popup will ask if the user has selected the correct trials for export and after confirming the popup the .txt file will be printed to `home/p3rtp/DVHtoTXT`. This .txt file can then be opened in excel and copied to the DVH QA spreadsheet. The left column is dose in cGy and the right column is volume in  $\text{cm}^3$ . In order to recreate the cumulative DVH shown in Pinnacle the user must make a column of relative volume by dividing the volume by the max volume for the ROI and plotting the dose versus the relative volume.

## **Appendix B – Requesting the DVH QA Spreadsheet**

If you are interested in obtaining a copy of the dose volume histogram Microsoft Excel spreadsheet please contact one of the following:

E. Ishmael Parsai, Ph.D., FACRO, DABR, DABMP

Department of Radiation Oncology

Professor & Chief of Medical Physics

Director of UT Graduate Medical Physics Program

[e.parsai@utoledo.edu](mailto:e.parsai@utoledo.edu)

Or

Diana Shvydka, Ph.D.

Department of Radiation Oncology

Assistant Professor

[diana.shvydka@utoledo.edu](mailto:diana.shvydka@utoledo.edu)